

Florida Institute of Technology

Scholarship Repository @ Florida Tech

Theses and Dissertations

5-2020

Design, Analysis, and Demonstration of a Multipurpose Fluid Tank Dynamics Characterization Platform

Cameron Ian Hume

Follow this and additional works at: <https://repository.fit.edu/etd>



Part of the [Mechanical Engineering Commons](#)

Design, Analysis, and Demonstration of a Multipurpose Fluid Tank Dynamics
Characterization Platform

by

Cameron Ian Hume

A thesis submitted to the College of Engineering and Science of
Florida Institute of Technology
in partial fulfillment of the requirements
for the degree of

Master of Science

in

Mechanical Engineering

Melbourne, Florida
May, 2020

We the undersigned committee hereby approve the attached thesis, “Design, Analysis, and Demonstration of a Multipurpose Fluid Tank Dynamics Characterization Platform,” by Cameron Ian Hume.

Daniel Kirk, Ph.D.
Professor, Aerospace and Physical Sciences and Associate Dean
for Research
College of Engineering and Science
Thesis Advisor

Hector Gutierrez, Ph.D.
Professor, Mechanical and Civil Engineering

Munevver Mine Subasi, Ph.D.
Associate Professor
Mathematical Sciences

Ashok Pandit, Ph.D.
Professor and Department Head
Mechanical and Civil Engineering

Abstract

Title: Design, Analysis, and Demonstration of a Multipurpose Fluid Dynamics
Characterization Platform

Author: Cameron Ian Hume

Advisor: Daniel Kirk, Ph. D.

The development of a highly versatile multiphase fluid tank characterization platform is essential to the analysis and improvement of propellant storage tanks. The performance of these tanks is highly critical to the safety and performance of their carriers, especially in the space industry where the propellant makes up the overwhelming majority of the mass of the vehicle. This thesis outlines the design and development of a linear stage used to test and validate the characteristic of multiphase fluids inside moving specific tanks. This document will walk through the steps taken to bring a new linear stage to life, from the development of effective requirements, through design and analysis to the demonstration of the final product. The final product is a powerfully yet precise piece of machinery that will add value to the area of fluids research for years to come.

Table of Contents

Abstract	iii
Table of Contents	iv
List of Figures.....	vii
List of Tables.....	ix
Acknowledgments	x
Chapter 1 - Introduction	1
1.1. Background	1
1.2. Motivation	2
1.3. Objective	2
1.4. Approach.....	2
1.5. Thesis Overview.....	3
Chapter 2 - Literature Review	5
2.1. Review of the large Linear Stage	6
Chapter 3 - Requirements.....	7
Chapter 4 - Stage Design.....	10
4.1. Foundation.....	10
4.1.1. Emergency Containment Devices	12
4.2. Motion Interface.....	13
4.3. Drivetrain	16
4.3.1. Drivetrain Limitation.....	18
4.3.2. Drivetrain Power Delivery.....	19
4.4. Instrumentation and measurement	21
4.4.1. Force Sensors.....	21
4.4.2. Placement and Mounting.....	21
4.4.3. Stage Oscillation Measurement.....	22

4.4.4.	Stage Homing and Limits	22
4.5.	Moving Frame	24
4.5.1.	Lower Frame	24
4.5.2.	Upper frame.....	25
Chapter 5 -	Analysis	27
5.1.	Working load Analysis.....	27
5.1.1.	Lower Frame	27
5.1.2.	Analysis of Clevis.....	29
5.1.3.	Tuned Deformation of Upper Frame	31
5.2.	Emergency Containment Devices	34
Chapter 6 -	Fabrication	39
6.1.	Foundation.....	39
6.2.	Motor – Actuator Connection	40
6.3.	Lower Frame	41
6.4.	Linear Bearing and Rail Alignment	41
6.5.	Emergency Containment Device.....	43
6.6.	Upper Frame.....	43
Chapter 7 -	Calibration	44
7.1.1.	X-Force Calibration.....	47
7.1.2.	Y-Force Calibration.....	48
7.1.3.	Z-Force Calibration	49
7.1.4.	X & Y-Torque Calibration	49
7.1.5.	Z-Torque Calibration.....	51
Chapter 8 -	Demonstration	52
8.1.	Complete System Overview	52
8.2.	Human-Machine Interface	54

Chapter 9 - Conclusion and Future Work.....	55
References	56
Appendix - Actuator Alignment.....	2

List of Figures

Figure 1: Large Linear Stage.....	6
Figure 2: Drivetrain Monitoring Thermometer	8
Figure 3: Linear Stage Overview	10
Figure 4: Foundation Dimensions (units: mm)	11
Figure 5: Emergency Containment Device Layout	12
Figure 6: Center of Gravity Locations in X-Z Plane.....	14
Figure 7: X Location of Centers of Gravity	15
Figure 8: Kollemorgan AKD Servo Drive	19
Figure 9: Kistler 9047B 3 Axis Force Sensor	21
Figure 10: Isometric overview of Lower Frame.....	24
Figure 11: Lower Frame Overview	25
Figure 12: Deformation of Lower Frame	28
Figure 13: Von-Mises Stress in Lower Frame	28
Figure 14: Clevis and Spherical Joint Layout	29
Figure 15: Clevis Load Analysis Configuration.....	30
Figure 16: Clevis Deformation Under Load.....	30
Figure 17: Von-Mises Stress in Clevis Under Load.....	31
Figure 18: Upper Frame Load Analysis Configuration.....	32
Figure 19: Upper Frame Deformation Under Load.....	33
Figure 20: Emergency Containment Device Analysis Loading Configuration.....	36
Figure 21: Emergency Containment Device Deformation Under Load.....	37
Figure 22: Von-Mises Stress in Emergency Containment Device Under Load.....	37
Figure 23: Preparation of Foundation for Concrete Slab	39
Figure 24: Motor-Actuator Connection Undergoing Annealing	40
Figure 25: Foundation with Linear Rails Mounted and Secured.....	42
Figure 26: X-Force Calibration Setup	47
Figure 27: Y-Force Calibration Setup	48
Figure 28: Z-Force Calibration Setup.....	49
Figure 29: X and Y Torque Calibration Setup	50
Figure 30: Z-Torque Calibration Setup	51
Figure 31: Complete Linear Stage Overview.....	52

Figure 32: Completed Linear Stage Front View	53
Figure 33: Completed Control and Instrumentation Panel.....	53
Figure 34: HMI Main Navigation Screen.....	54
Figure 35: HMI Automated Stage Controls	54
Figure 36: Overhead View of Indicator.....	2
Figure 37: Drivetrain Alignment Bolts.....	3

List of Tables

Table 1: Table of frequency vs amplitude requirements 8
Table 2: Upper Frame Load Cell Support Deflection under Load 33
Table 3: Initial Alignment Figures 3

Acknowledgments

I would like to acknowledge my advisors, Dr. Daniel Kirk and Dr. Hector Gutierrez for guidance throughout this project. The staff and faculty at Florida Tech, with notable mention to the staff of the Florida Tech Machine Shop, for all the hard work behind the scenes that make projects like this possible. Colleagues that shared this project for their hard work and dedication, and friends and family for their continued support and encouragement throughout my education.

Chapter 1 - Introduction

1.1. Background

A rocket's weight at launch may consist of upward of 95% liquid propellant. This large mass fraction of liquid makes it vitally important to know and understand the dynamics of how the fluid will react to the movement of its surroundings. In particular, it is important to know the resonant frequencies and how to control and manipulate them.

In the 1950s NASA began working to understand more about the behavior of multiphase fluids in dynamic systems; however, scientists and engineers were limited to experiments and analytical equations to develop simple models that predicted response for simple geometries. The advent of more powerful computers changed all that. From the '80s onward computers began solving Computational Fluid Dynamics models that allowed insight into increasingly more and more complex models as the rise in computing power permitted.

Despite high powered computers being able to solve increasingly more complex models of dynamic systems, a large amount of money and effort are still being directed to validating these results using physical models. As such, the Florida Institute of Technology is developing a highly versatile platform to characterize a wide array of tank sizes and form factors over a broad range of test parameters.

During physical verification, a tank with similar geometry to that of the actual tank is placed on a linear stage and partially filled with a fluid of known characteristics. The linear stage is then used to oscillate the tank at a range of frequencies and amplitudes to develop fluid motion inside the tank. Cameras, 3D scanners, force sensors, and other measurement devices are then used to observe the response of the fluid within the tank. The observations of the physical model are then compared to results obtained from Computational Fluid Dynamics models to improve and to ensure their accuracy.

A linear stage is a piece of equipment used to produce very precise movement along a straight line. This movement is carefully controlled and used to induce or excite movement in the fluid within the tank to be analyzed. This movement can be used to simulate the effects of very different stages in the flight of a rocket, such as motion

induced by wind causing oscillation in the rocket while on the launch pad, known as pad sway, to investigating how fluid behaves during flight.

1.2. Motivation

Spacecraft are incredibly highly-strung pieces of modern machinery. Any unnecessary mass carried along in the form of redundancies or mass used to increase factors of safety carry a huge cost. In an interview, Tory Bruno, CEO of United Launch Alliance said: "...a factor of safety is really a factor of ignorance" (Bruno 2020). The motivation behind this research is to develop a piece of equipment that allows for a greater understanding and the verification of multiphase fluids in tanks under motion. This greater understanding allows engineers to reduce the ignorance involved in the design and development of space systems to reduce unnecessary costs while increasing safety.

1.3. Objective

A new linear stage needs to be built as a method for validation of Computational Fluid Dynamics simulation models of propellant storage tanks. The aim is to produce a highly versatile system that allows a large number of diverse tests to be carried out over its lifetime. The platform must be user friendly and easy to operate to allow for seamless collaboration between research members. The platform should also allow for simple design and fabrication of structures to support and test future models to be analyzed. The product must be reliable to ensure a long service life with minimal routine maintenance while ensuring the safety of the operators and all involved.

1.4. Approach

Upon being tasked with its development, the first step taken was to develop a clear set of requirements for the stage to fulfill. These requirements were not only based on current needs but also included significant thought into the needs of future models.

Once a clear set of requirements had been laid out, design began on the linear stage. The design process looked at several different configurations of linear stages as well as different methods for driving the linear stage. From here on an iterative design process was used. A design was drafted and subsequently reviewed by a team with knowledge in the field. If no major design flaws were found, then the design would move on to

Finite Element Analysis (FEA). During FEA the model was tested at working load to check deformation under ordinary conditions and under high loads to verify the safety of the device. As these analyses were performed, modifications were made to the stage and the cycle repeated until a final stage design was settled upon.

Construction took place with a variety of vendors and sources of components working together to complete the stage in a timely manner. Once physical construction had been completed, the drive components of the stage were then programmed and the machine was ready to begin operation.

1.5. Thesis Overview

This thesis will cover the process of the development of a new, highly versatile linear stage from design right through to demonstration. The thesis will begin with a review of similar linear stages being used to conduct research and have a look at the shortcomings of some of these linear stages. Chapter 3 will then present the requirements that the new stage was built to achieve to remedy several of these shortcomings.

Chapter 4 will outline the design process that led to the final design solution as well as some alternative solutions that we considered, but did not select. A more detailed final solution that looks at each segment of the design and discusses design choices will then be presented.

As safety is a high priority, a thorough analysis of the stage was performed to ensure proper function and to verify that safety devices will perform as expected in the event of a loss of control. These analyses also serve to verify the structural rigidity of the linear stage that is vital to the proper performance and accurate, repeatable data acquisition.

Chapter 6 will present a walkthrough of the fabrication procedure used to take the design to a working final product. This section will pay particular attention to areas of the fabrication that required greater attention to detail due to the tight tolerances involved in the alignment of moving components.

Calibration is an essential part of the process that required careful consideration development to a system that was capable of accurately and repeatably calibrating the system with a variety of different tanks and structures.

Chapter 8 presents the results of the hard work and dedication that went into the development of the final products and demonstrates the capabilities of the finished system. Final remarks are made in chapter 9 including an outline of future work to be performed using the linear stage.

Chapter 2 - Literature Review

The field of multiphase fluid tank characterization has been under investigation by NASA since the 1950s and gaining momentum through the 60s as the space race heated up. Dozens of papers were released during this time that showcased the techniques in use at the time. A great collection of these can be found in an updated version of NASA's SP-106 (Abramson 1966) that compiles much of the original information but has been updated for the sake of clarity and accuracy. The new "Dynamics Behavior of Liquids in Moving Containers" (Dodge 2000) is a treasure trove of valuable information in this field.

More recently, the field of Computational Fluid Dynamics has allowed a deeper investigation into this field; however, these results still require verification from physical tests to ensure accuracy. Experimental and Numerical Investigation of Liquid Slosh Behavior Using Ground-Based Platforms (Ran Zhou 2012) presents a compelling example of physical analysis being used alongside CFD.

The Florida Institute of Technology in conjunction with Orbital ATK, now Northrop Grumman Innovation Systems, had previously invested in the development of a linear stage (G. Lapilli 2016) at FIT's Center for Advanced Manufacturing and Innovative Design (CAMID) known as the Large Linear Stage and has been in use ever since. However, the needs of research have fast outgrown the capabilities of this linear stage leading to the development of a linear capable of performing tests on larger tanks at higher frequencies.

While the validation of slosh characteristics is vitally important of spacecraft, slosh characteristics testing and verification also find their place in much more terrestrial applications. In the article, "Investigation and Development of Fuel Slosh CAE Methodologies", (Vaishnav 2014) Vaishnav et al investigate the slosh in vehicle fuel tanks and its effects noise, fuel supply at low fill levels and failure due to high impact forces. Tests similar to these may be carried out on the linear stage presented in this thesis however we will direct the focus from here on to the analysis of spaceflight hardware.

2.1. Review of the large Linear Stage

The large linear stage was designed and built at the Florida Institute of Technology and began testing in May of 2016. The system was designed for testing large spherical or pill-shaped tanks up to 50 inches wide and 100 inches tall with mass as high as 2,000kg. This platform has a maximum stroke length of 15 inches and a maximum operating frequency of 1.5 Hz

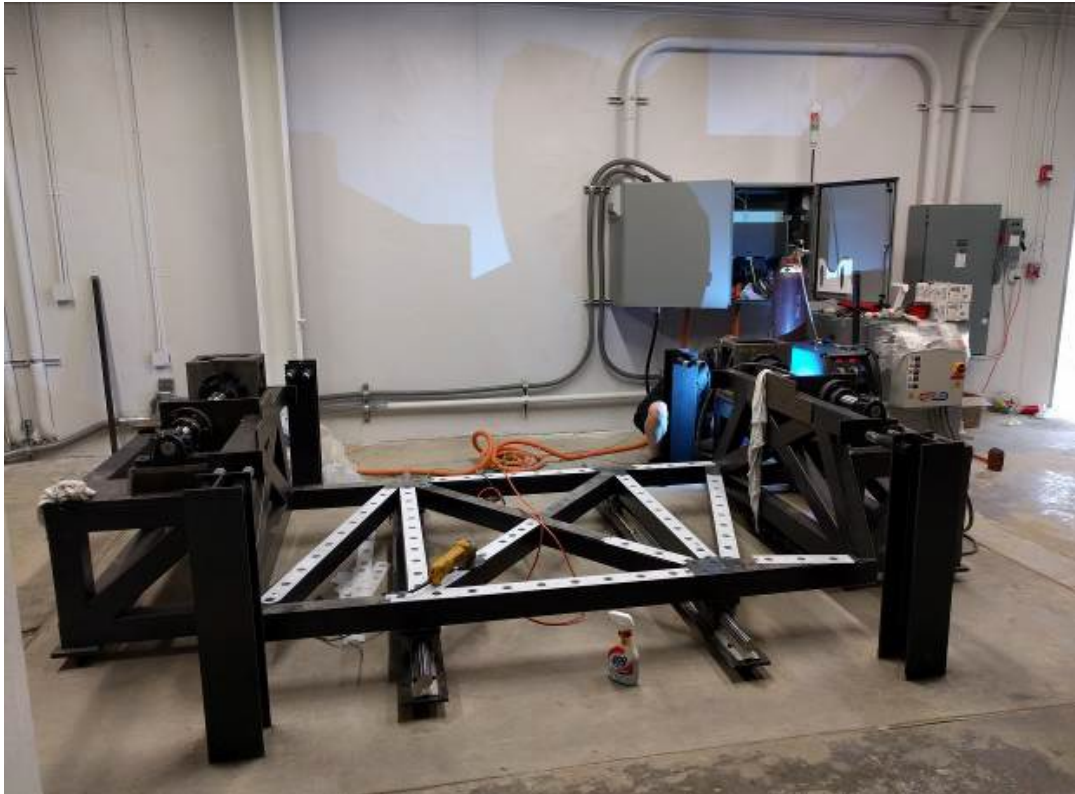


Figure 1: Large Linear Stage

This platform utilized a pair of Siemens 1PH8 Synchronous servomotors each rated at 100 hp powering a 64mm SKF lead screw and had an expected lifespan of 20,000 hours.

Chapter 3 - Requirements

Defining a clear, well thought out set of requirements lays a solid foundation on which a project is built, and this project was no exception. The requirements for this project were initially guided by the immediate needs of a pair of projects waiting to undergo a series of tests that were unable to be completed on the linear stage present and already in operation (G. Lapilli 2016) as the needs of the tests were beyond its capabilities.

A study was then conducted that looked at verification simulations of multiphase fluid storage vessels and defined a broad set of desirable parameters. These parameters were then further used to guide the requirement development process.

It was decided that the target moving mass requirement would be set at 3600kg this mass included any hardware attached to the stage that contributed to the moving weight. This included all frames, supports and measurement devices.

Another key aspect of the design of the linear stage is the operational stroke length of the machine. However, these criteria were more complex than initially anticipated. Early on in the design process, it was discovered that a pair of linear rails remained as surplus from repairs made to another linear stage. These linear rails proved to have ideal loading characteristics for use in the upcoming linear stage however were already cut to length. This length restriction created a trade-off situation between the operational stroke of the machine and the product of mass and center of gravity of the load to be tested. The end result of this trade-off concluded to set the maximum stroke length of 0.4m travel from end to end.

During a standard sinusoidal analysis of a tank, the speed and acceleration are controlled as a function of the amplitude and the frequency at which the stage oscillates. This leads to a requirement that drives two highly important characteristics of the platform. More importantly, the speed and acceleration are driven by the product of the frequency and amplitude of the oscillations. This gives rise to a situation where we cannot define independent requirements for the frequency and amplitude of the stage. To deal with this interdependency the requirements for the frequency are given as discrete points of matched pairs of amplitude and frequency. The chosen values were as follows:

Table 1: Table of Frequency vs Amplitude Requirements

Amplitude (m)	0.2	0.1	0.005
Frequency (Hz)	0.75	1.2	2

As well as sinusoids, the stage is also expected to be able to perform several other types of maneuvers including, but not limited to step functions, swept-frequency sinusoids, sawtooth waves, and superpositions of sinusoids.

During operation, the machine is expected to produce an unsustainable amount of heat due to inefficiencies in the system. Although measures can be taken to remove heat from the system using water cooling or similar methods, it was decided that these measures are not necessary. This is because the vast majority of tests of this nature are short-duration test that lasts a few minutes before coming to rest. This rest period will allow the system to cool before being tested again. This heating and cooling cycle, known as a duty cycle, was set as a requirement for the design. The duty cycle requirement was chosen to have a maximum required cycle run time of 5 minutes followed by as little as a 5 minute cool-down period after every cycle. These parameters represent a maximum of a 50% duty cycle with a period of 10 minutes. While running under lower loads the machine will be capable of exceeding the 5 minute run time. This results in the temperature of the motors and actuators need to be monitored during longer tests. To do this a set of thermometers will be used to monitor the temperature during operation. The maximum allowable temperature for the motors and actuators is 120°C (Kollmorgen n.d.) and 70°C (Thomson Linear n.d.) respectively. A thermometer such as the magnetic-backed thermometer below available at McMaster-Carr item 3982K14 can be used to continuously monitor the drivetrain.



Figure 2: Drivetrain Monitoring Thermometer

Safety was of utmost importance during the development of the linear stage and as such, several requirements were laid out early on in the process. The first safety requirement laid out was the inclusion of an easily accessible emergency stop button that would decelerate the stage as quickly as possible to a standstill before powering down the motors. This safety feature is important in the event that the operator notices something that necessitates the immediate shutdown of the machine.

The second major safety requirement describes the implementation of a means to physically restrain the stage in the case of a failure. These emergency containment devices must be able to prevent the linear stage from exceeding its normal area of operation under worst-case loading under several different scenarios. These scenarios consist of mechanical failure of any component including internal components of the actuators, linkages between the actuators and lower frame. Another concern was the loss of control of the actuators due to errors in the software or electrical failure.

Chapter 4 - Stage Design

The final design of the linear stage shown below represents the culmination of months of design work and analysis iterated to produce a design that fulfilled all the requirements laid out in the previous chapter. The image below shows the linear stage fitted with the optional upper frame which acts as a multipurpose adapter for a wide variety of tank slosh applications.

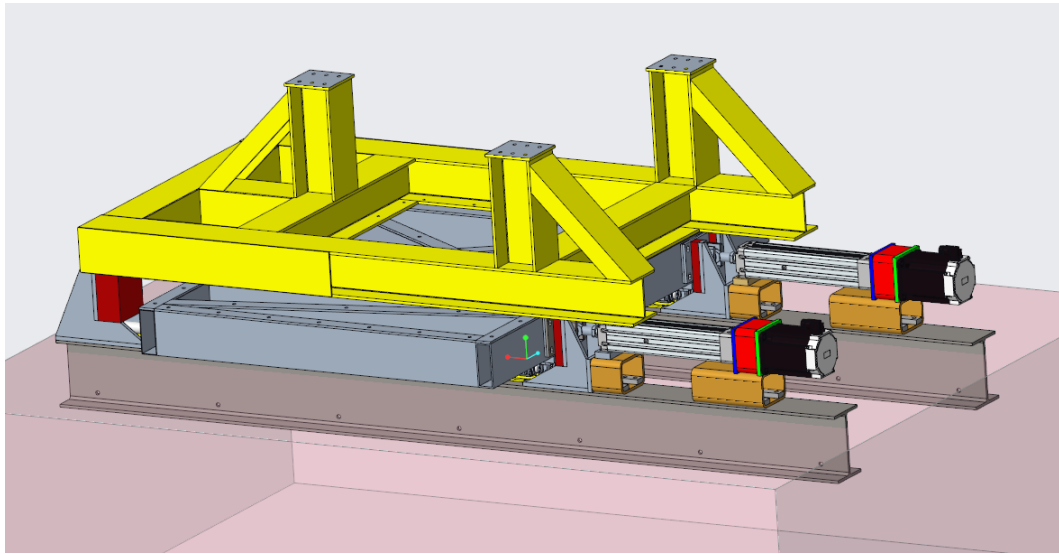


Figure 3: Linear Stage Overview

The design of the linear stage can be separated into 5 distinct segments: the foundation, moving frame, motion interface, drive train, and instrumentation and measurement. The foundation consists of the non-moving parts of the system, starting with the concrete foundation up to the linear bearings. The moving frame segment consists of all the moving components in the system that are not used to drive the linear stage and the drive train is all components used to drive the linear stage. The drivetrain consisted of all the components needed to induce motion in the stage from the ball screws back through to the motor drives. All components used to take measurements or recordings of an analysis performed on the linear stage are covered under instrumentation and measurement.

4.1. Foundation

The foundation of the system serves as an anchor to the stage. As the stage is forced back and forth it produces a net force that needs to be restrained. A large concrete slab

provides sufficient support to restrain this residual force. The reinforced concrete slab has a width of 3.15m, length 4.32m, and depth 1.22m, this results in a foundation weighing approximately 39.6 metric tons.

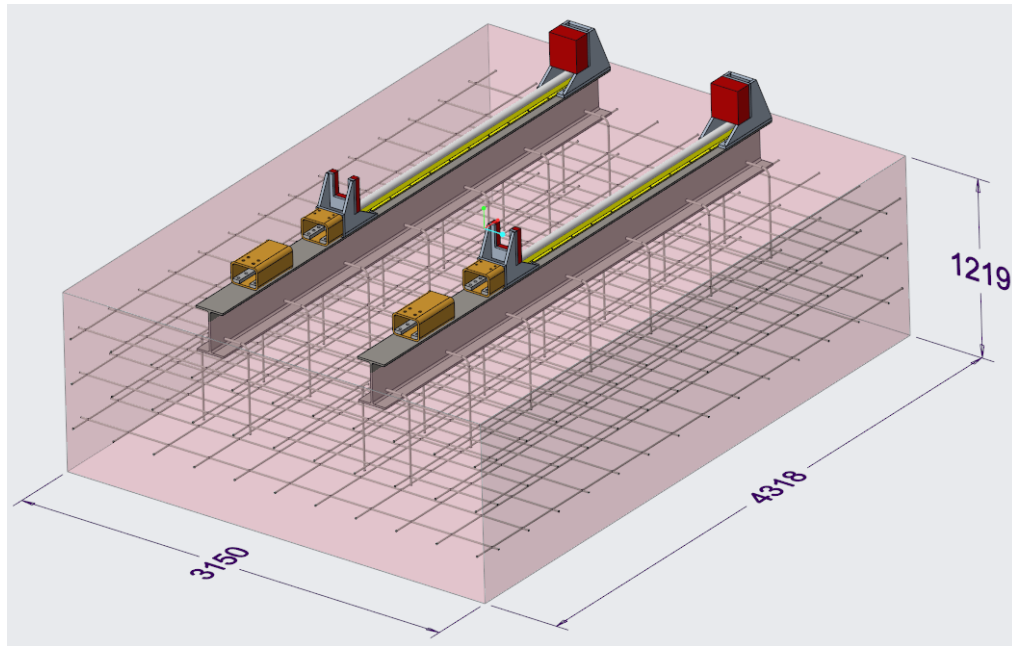


Figure 4: Foundation Dimensions (units: mm)

The foundation also serves to eliminate any vibrations that may be imparted on the surrounding building. In order to eliminate the vibrations, the slab is isolated from the surrounding building through a 20mm rubber pad. This pad also allows for thermal expansion and contraction of the slab and surrounding building without damage.

The interface between the linear stage and the foundation slab is a pair of 12 inch I-beams that span nearly the length of the slab. These I-beams are embedded 225mm within the slab allowing for space beneath the upper flange to access the hardware to attach the rest of the components. The beams are also supported by a series of reinforcing tie bars that are threaded through holes which are drilled through the web of the beam. These reinforcements provide additional strength in the bond between the beam and the slab.

These beams serve as the primary mount for the rest of the components, thus it is important that the beams are straight, flat and level. Several procedures were performed

prior to and during the installation of the beams to ensure that the beams were straight, flat and level. These details are discussed in further detail in Chapter 5 during fabrication.

The hardened steel linear rails upon which the stage will traverse are supported by an extruded aluminum support, which is intern mounted directly to the embedded beams. It is vital that these rails are mounted parallel to prevent excessive loading on the linear bearings which may cause binding and premature failure.

4.1.1. Emergency Containment Devices

In the event of an emergency due to mechanical failure or loss of control of the actuators, there needs to be a system in place that will contain the stage within its working are. The solution to this problem was chosen as a firm end-stop at the outer limit of travel on each end of the linear rails. These structures are comprised of heavy steel plates welded into a triangular gusset. These gussets provide sturdy support for a block of rubber placed at the contact surface between the stage and the gusset. The blocks of rubber create a layer 114mm thick that acts as an energy absorption device in the unlikely event the stage collides with these containment devices.

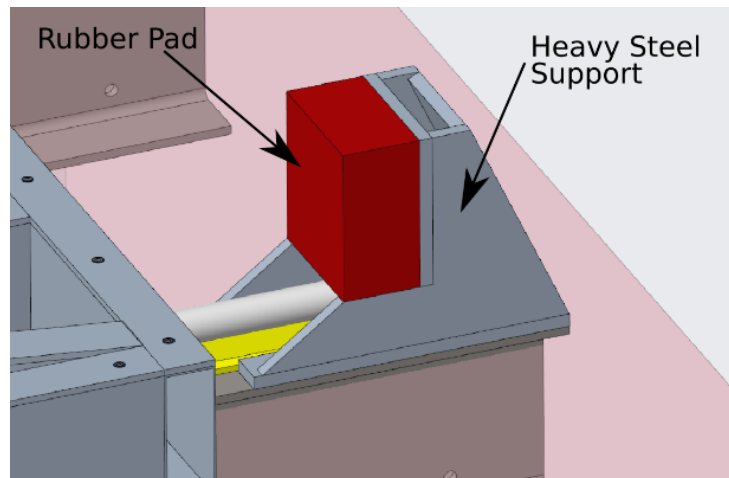


Figure 5: Emergency Containment Device Layout

4.2. Motion Interface

The motion between the moving platform and the foundation is facilitated by the use of recirculating ball bearings. These bearings utilize a set of trapped ball bearings that are recirculated through a track housed inside a hardened case. These bearings allow for continuous motion along a hardened rail under high loading with minimal friction and wear.

The bearings chosen for this application are the SKF LUCT 50 BH, that ride on a pair of precision 50mm hardened steel supported shafts. Each of these bearings provides support for a maximum static load of 17 000N and a maximum dynamic load of 17 300N (Thomson Linear n.d.). The stage will utilize a pair of linear bearings mounted on each corner of the stage

It is important to note that these bearings are not designed to carry any negative vertical force, which is a force pulling them off the linear rail.

In order to calculate the force applied to each of the linear bearings, we need to note that the center of gravity and location of the driving forces are located above the bearings. This will create a torque about the stage during acceleration. Thus, in order to calculate the total force on the bearings, we need to calculate the force due to this torque in addition to the weight due to gravity. We are able to calculate the force F_{τ} applied by the acceleration torque using the following formula:

$$F_{\tau} = \frac{Acc}{D_{Bearings}} (Z_{Load} * M_{Load} + Z_{Stage} * M_{Stage} - Z_{Driving Force} * (M_{Stage} + M_{Load}))$$

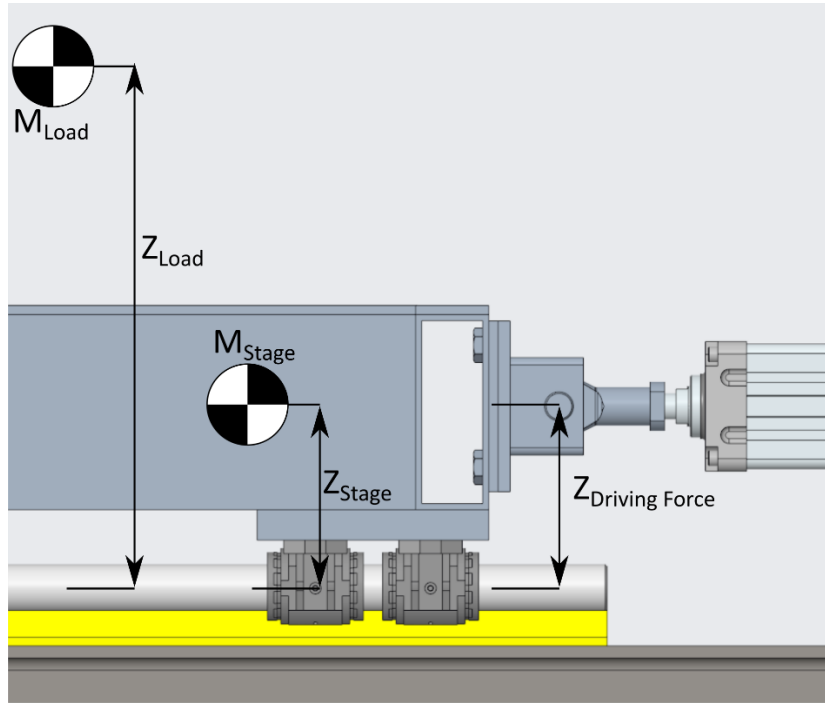


Figure 6: Center of Gravity Locations in X-Z Plane

Where Acc is the maximum acceleration of the stage, $D_{bearings}$ is the horizontal distance between the bearings, Z_{Load} and Z_{stage} are the vertical distance from the center of the bearings to the center of gravity of the load and stage respectively, M_{load} is the mass of the load to be tested, and M_{stage} is the mass of the stage. $Z_{Driving\ force}$ is the vertical distance between the center of the bearing and the point the stage is being forced from.

The force on the bearings due to the weight of the stage is proportional to the weight of the stage and its load and the distance from the center of gravity of the components to the center of the bearing clusters.

$$F_{g1} = g * (M_{Load} * \frac{X_{Load}}{D_{Bearings}} + M_{Stage} * \frac{X_{Stage}}{D_{Bearings}})$$

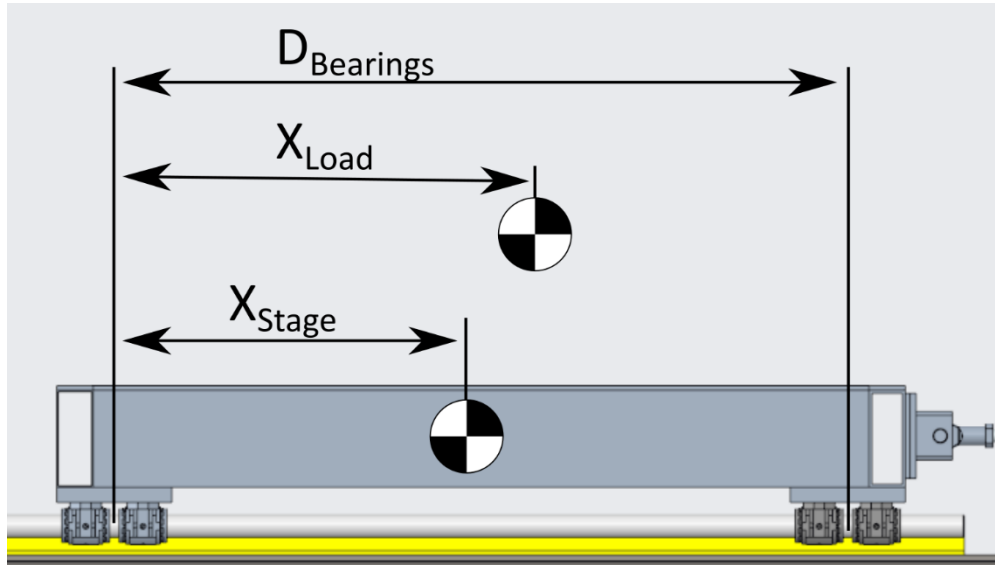


Figure 7: X Location of Centers of Gravity

Where X_{Stage} is the distance from the center of gravity of the stage and g is the acceleration of gravity. X_{Load} and X_{Stage} are the distance in the X direction of the center of masses of the load and stage respectively. This equation allows us to calculate the force due to gravity on one end of the stage; however, since we are concerned with the loading on the bearings on both ends of the stage, it is important that we account for both ends of the linear stage.

$$F_{g2} = g(M_{Load} + M_{Stage}) - F_{g1}$$

We account for the acceleration of the stage being either positive or negative in the calculation on the total loading on each of the four bearings on each end of the stage

$$F_{Bearing} = \frac{F_{g1,2} \pm F_t}{4}$$

Given the force on each bearing, it is important to note that the bearing will fail if $F_{Bearing}$ is either greater than the maximum dynamic loading of 17000N recommended by SKF or becomes negative. With this, we can begin to form the limits of the stage as a function of the mass and positioning of the load as well as the maximum acceleration.

It is important to note that these calculations are made with the assumption that the mass distribution is symmetric about a plane perpendicular to the direction of gravity and

located equidistant from each of the linear rails. If this assumption cannot be made, then this will result in significant torques being generated resulting in sideways loading of the bearings. This may result in premature failure of the bearings.

4.3. Drivetrain

The drivetrain that was chosen to power the system consists of a ball screw driven through a coupling by a servo motor. In order to verify the drivetrain is capable of effectively and safely driving the system, we need to closely examine the limits of each component. More specifically, to ensure the servo motor is capable of developing enough torque throughout the operating range and the ball screw is capable of converting the torque generated to linear force.

The motor is responsible for converting electrical power to the motion of the system. However, at a closer look, there are several intermediate power transferring components that need to be accounted for, particularly when investigating the acceleration of the system.

A given sinusoidal motion profile can be decomposed into equations.

$$x = A\sin(\Omega t)$$

$$v = A\Omega\cos(\Omega t)$$

$$a = -A\Omega^2\sin(\Omega t)$$

Where A is the amplitude, Ω is the excitation frequency of the stage in rad/s .

Next, the force required to drive the stage is calculated by

$$F = ma + \mu_d mg$$

Where m is the mass of the moving stage and μ_d is the dynamic coefficient of friction between the linear rails and bearings as estimated by the manufacturer (SKF) (SKF 2014).

Converting to rotational motion:

$$\theta = \frac{2\pi x}{l}$$

$$\omega = \frac{2\pi v}{l}$$

$$\alpha = \frac{2\pi a}{l}$$

$$T_{driving} = \frac{l}{2\pi} \frac{F}{0.9}$$

Where l is the advance of the lead screw per revolution and 0.9 is assumed to be a conservative estimate of the efficiency of the conversion of rotational torque to linear force.

The torque required can be calculated by the following equation:

$$T_{total} = T_{internal} + T_{driving}$$

Where $T_{internal}$ is the torque required to overcome the inertia under the rotational acceleration of the motor and lead screw components.

$$T_{internal} = \alpha(I_{screw} + I_{coupling} + I_{motor})$$

Where I_{motor} is given by the manufacturer, $I_{coupling}$ is assumed to be negligible and I_{screw} is calculated as follows:

$$I_{screw} = \frac{\pi}{32} \rho L D^4$$

Where ρ is the density of the lead screw material, L is the length of the shaft and D is the shaft diameter.

The motor power can now be calculated:

$$P_{total} = T_{total} \omega$$

4.3.1. Drivetrain Limitation

In order to ensure safe operation of the linear stage, a set of important safety checks need to be conducted on the intended excitation pattern. These checks ensure that none of the ratings of each component is exceeded.

The relevant checks for the servo motor are:

- $\max(\omega) * 60/2\pi > \max RPM$
- $\max(T_{total}) > peak\ torque$
- $\max(P_{total}) > rated\ power$
- $rms(T_{total}) > \max\ continuous\ torque$

The relevant checks for the actuator are:

- $\max(T_{total}) > \max\ actuator\ shaft\ torque$
- $\max(F) > \max\ actuator\ X - Force$
- $\max(\omega) * 60/2\pi > \max RPM$

If any of the above conditions are met, then the intended excitation plan is beyond the safe operating limits of the system and should not be performed.

From the analysis above it is determined that the height of the center of gravity of the stage is most likely to be the limiting factor during tests. For this reason, it is highly recommended that the design of any structure to be tested on the linear stage be optimized to achieve as low of a center of gravity as possible. It may also be noted that if the design necessitates a center of gravity are high enough to cause concern with the bearing lift-off restriction, then a mass can be added low on the linear stage to effectively lower the center of gravity of the moving portion of the stage provided the maximum weight limit is not exceeded.

4.3.2. Drivetrain Power Delivery

The drivetrain power delivery system supplies a carefully controlled amount of power to the system in response to operator command and motor position feedback. Starting from the 480V AC mains input to the system the power is first controlled by a manual contactor. After this, the power is passed through a choke that prevents high frequencies from being fed back into the mains supply. The power is then passed to a pair of Kollmorgen AKD servo motor drives, these drives are responsible for controlling the power being fed to the motors. These drivers are capable of delivering a continuous current of 72 Amps and a peak power of 140 Amps.

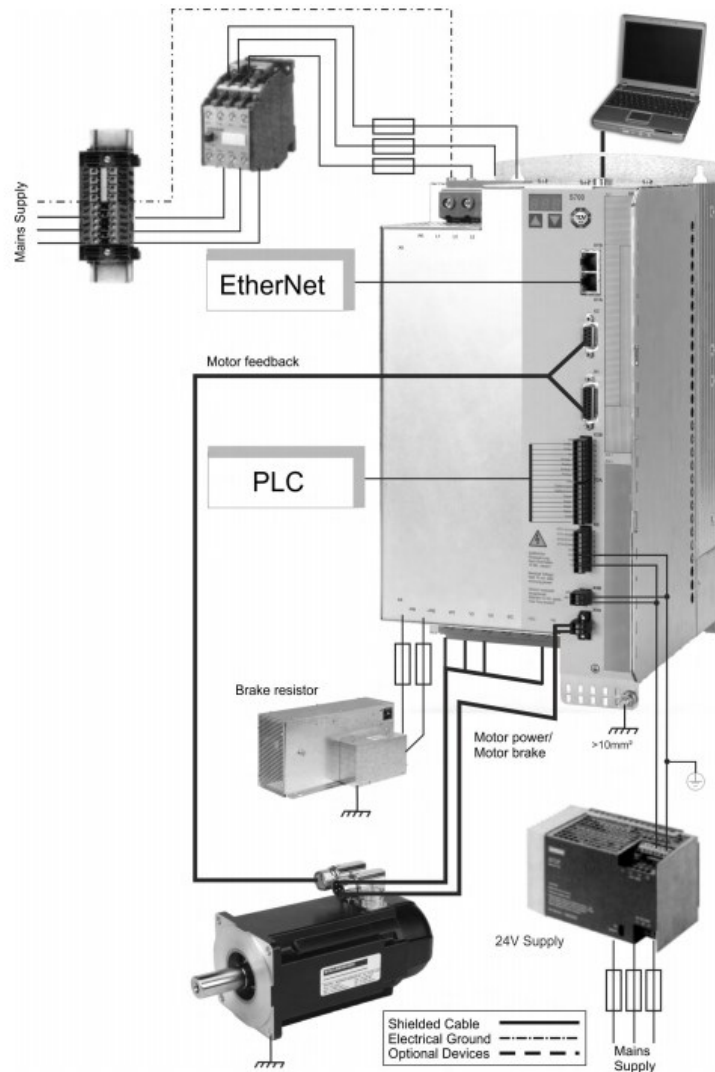


Figure 8: Kollmorgen AKD Servo Drive

At times during the operation of the linear stage, particularly during hard deceleration, the Servo drives need to be able to dump power from the system. This is done using a pair of braking resistors that are used to convert excess electrical power into heat to be dissipated. Each braking resistor is capable of continuous power dissipation of 3kW and a peak power dissipation of 4.8 kW.

4.4. Instrumentation and measurement

4.4.1. Force Sensors

The platform is primarily designed to operate using one of two sensor packages depending on load and test configuration. Both configurations utilize three piezoelectric 3-component force sensors provided by Kistler, namely the 9047B and the 9465B. These force sensors contain 3 pairs of quartz plates arranged such that each pair is sensitive to force in the three orthogonal directions.



Figure 9: Kistler 9047B 3 Axis Force Sensor

Depending on the force applied to a positive or negative charge will be developed. The polarity and magnitudes of this charge are used to calculate the magnitude and direction of the force applied to each of the three pairs of crystals.

4.4.2. Placement and Mounting

Each sensor is packaged into a square toroidal housing where the force is measured between the upper and lower surfaces. These surfaces need to be in constant contact with load applying surfaces and cannot experience or measure any tension applied to the face. In order to deal with this, each sensor package is placed between two parallel plates that are preloaded by means of a bolt that passes through the center of each toroid, thus the tension force in the Z direction is measured as a reduction in the preload force. These bolts are tensioned to apply predetermined force, which is discussed in more detail during calibration.

The transverse shear forces are again applied to the faces of the package; however, these components rely on the friction between the face of the package and the surface applying

the load. It is important for the transverse force not to exceed the maximum static friction applied by the preload and any additional force applied to the package.

In order to be able to apply the high preloading required to fulfill these requirements the force sensors needed to be mounted to a material that is significantly harder than the mild steel used for the majority of the stage. The material chosen for this application was 316 stainless steel, as its properties combined the necessary hardness with reasonable machinability.

4.4.3. Stage Oscillation Measurement

To ensure the stage is oscillating as expected it is important to incorporate a feedback system that allows the user to retrieve data about the true movement of the stage. This data will be used to compare the true movement of the stage to the commanded movement of the stage. This data will be used to adjust the gains in the servo drive system in order to improve the accuracy at which the drive system can follow the commanded signal. This data may also be used in the computer analysis to ensure the movement is each test is as similar as possible.

Each linear actuator has been fitted with an rotary resolver that monitors and records the movement of each actuator to take this measurement. This information can then be retrieved from the control model to be used later.

It is important to note that the rotary resolver does not measure the true position of the linear stage but rather measures the position of the motor. This allows the possibility that small errors may be incurred due to play or slop in the system, however, these errors will be small and have been deemed to be negligible for the purposes of this stage

4.4.4. Stage Homing and Limits

While the linear stage is capable of measuring relative position over its operating range, it has no way of directly measuring where it is in its range. In order to achieve this, a set of three inductive proximity sensors will be used to help locate the stage in its range and prevent it from exceeding its normal operating range. A single inductive proximity sensor will be used to denote the home position, this will be placed in the center of the operating range. When the machine is initiated the operator will start a homing cycle this

cycle while locating the central homing sensor and set its internal position to zero. From this point on, the controller will integrate to velocity in either direction over time to be able to assess its position.

An additional pair of inductive sensors will be placed at the extremes of the range of the machine. These sensors will be used to help prevent the stage from exceeding its normal operating range. If one of these sensors is triggered the stage will be brought to an immediate halt to prevent a collision with the emergency containment devices.

4.5. Moving Frame

The moving section of the stage is comprised of two main components: the lower frame and the upper frame, also referred to as the multipurpose frame. These components provide the necessary strength to support the test apparatus during the analysis as well as the necessary rigidity to ensure the measurements taken during the analysis are accurate and repeatable.

4.5.1. Lower Frame

The lower frame is designed to be a permanent feature of the stage that will be common for all tests and applications. The primary purpose of this frame is to act as a link between the linear bearings, linear actuators and the frame that supports load to be tested. This frame is also important, for it acts as the primary load transfer agent between the linear rails, linear actuators, and the load to be tested.

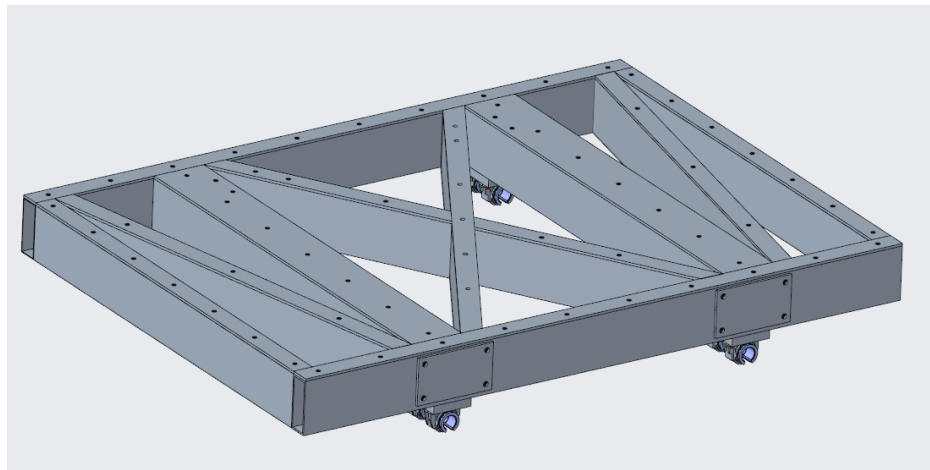


Figure 10: Isometric overview of Lower Frame

The low frame was designed using closed box sections that provided the high rigidity and strength needed while easing manufacturability. The frame consists of two main sections that are the primary load-bearing sections for the linear rails and linear actuators. These sections are triangulated to distribute the load across the stage.

4.5.2. Upper frame

The upper frame is designed to accommodate a large variety of testing needs to help reduce the time and cost of setup of future tests. However, this frame is also removable to reveal the flat platform of the lower frame which can accommodate for tests that are not suitable for the multi-purpose frame.

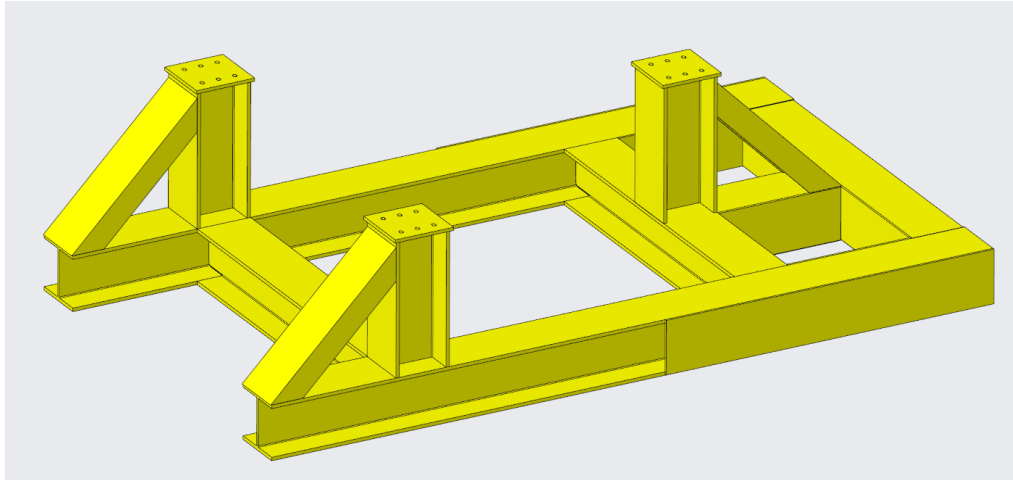


Figure 11: Lower Frame Overview

In order to ensure the versatility of the multipurpose frame, it had to meet several requirements. Primarily, the frame had to be strong enough to be able to support tanks up to the largest foreseeable tank without any risk of failure. Another important aspect of the design was the need to maintain clear visibility of the tank internals. An important metric in the testing of slosh characteristic is the visual interpretation of wave heights; therefore, unobstructed visibility both in the forcing direction and perpendicular to the forcing direction is essential.

The tuned deflection of the force measurement points is also an important aspect of the design of the multi-purpose frame. Although the physical deflection of the force measurement points is very small, on the order of a few tenths of a millimeter under working loads, it is still important that each force measurement point maintains the same stiffness. Consider that the force measurement devices are predominantly ceramic components with very high stiffness, they are very unforgiving to small deflections in relation to each other in a system. During high forcing conditions if a single force measurement mount was to be significantly stiffer than the others in the system, then

that sensor would be subject to a much larger proportion of the load. This could result in the premature overloading of a particular device and greatly limiting their maximum capacity as a system.

Chapter 5 - Analysis

5.1. Working load Analysis

The purpose of the working load analysis is to investigate the effect of the loads generated during operation. These loads are calculated by looking at expected future test and creating an assessment using the largest loads expected.

5.1.1. Lower Frame

The lower frame is the largest single component of the linear stage and is responsible for maintaining and directing the loads from several different components. The primary load carried by the lower frame is the transmission of force from the upper frame to the linear bearings. It is essential that the lower frame is able to transmit this for minimal deformation to protect the linear bearing from uneven loading that may result in premature failure. The polar moment of inertia in the X-Y plane is particularly low due to the planar design of the lower frame to maximize its versatility. To help combat this, taller box sections were used than previously intended. To verify that this and other bending modes of the frame will not become an issue during use, several loading scenarios were analyzed using ANSYS.

The analysis presented below examines the effect of a torque about the Y-axis that would be produced during the acceleration or deceleration of a test mass with a center of gravity well above the contact point. The moment was applied to the area lower frame that is contacted by the upper frame. The frame was fixed to the ground using cylindrical supports that mimic the reaction forces provided by the linear bearings. The results of this analysis are shown below.

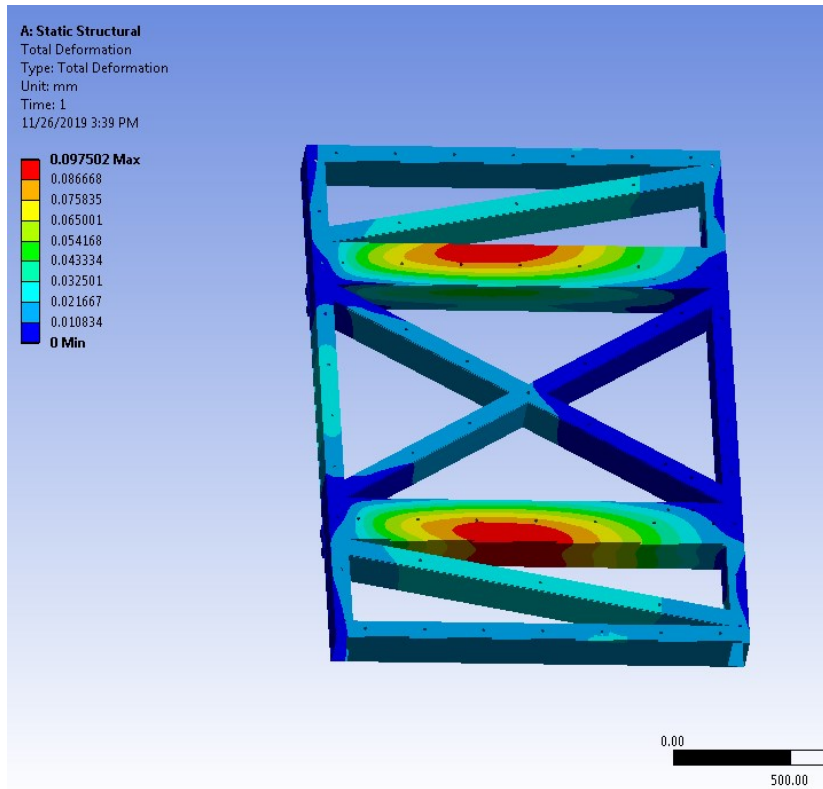


Figure 12: Deformation of Lower Frame

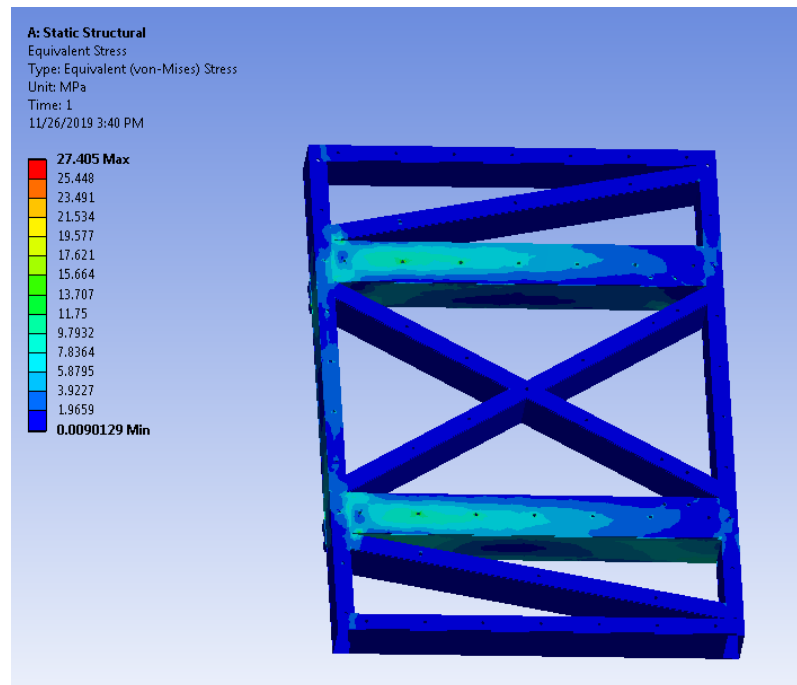


Figure 13: Von-Mises Stress in Lower Frame

Despite the reduced polar moment of inertial in the X-Y plane, the lower frame is still capable of transmitting the loads while only demonstrating small deflections and maintaining stresses well below the yield stress.

5.1.2. Analysis of Clevis

The clevises are responsible for transferring force from the linear actuators to the lower frame. It is imperative that these devices do not fail during operation, for a failure would result in a collision between the lower frame and the emergency containment devices.

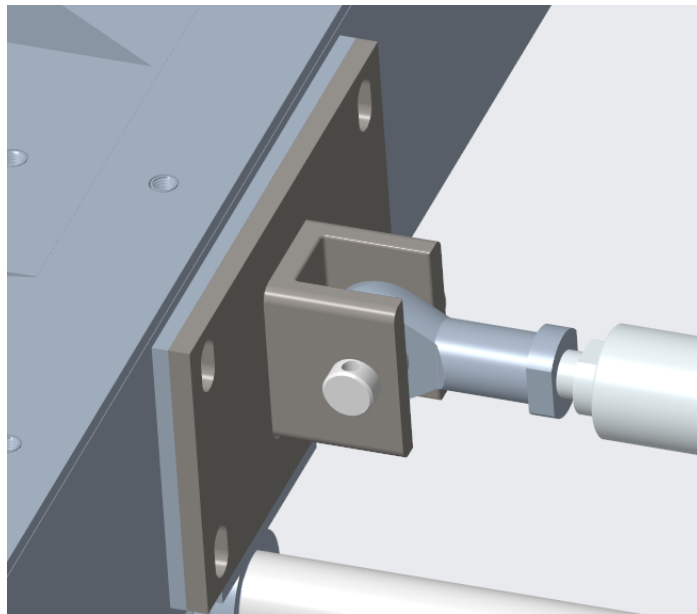


Figure 14: Clevis and Spherical Joint Layout

The clevis connects to the linear actuator through a spherical ball end that is located by means of a retained pin.

To verify the integrity of the clevis FEA was performed on the clevis using ANSYS. The clevis was loaded along the inside surface of the pinhole and secured to the lower frame

using a fixed support. A load of 35 000N was then exerted in an outward direction, this setup can be seen below.

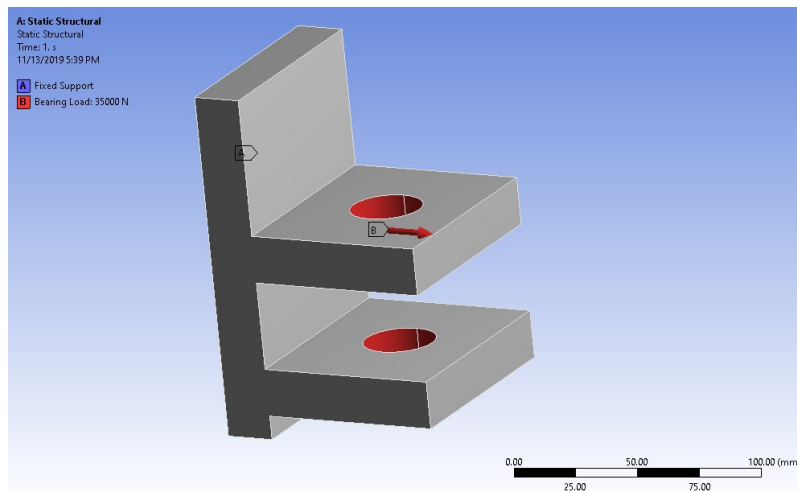


Figure 15: Clevis Load Analysis Configuration

The analysis showed minimal deformation in the clevis and resulting in equivalent stresses that are well below the yield stress of mild steel. The results of this analysis can be seen in the figures below.

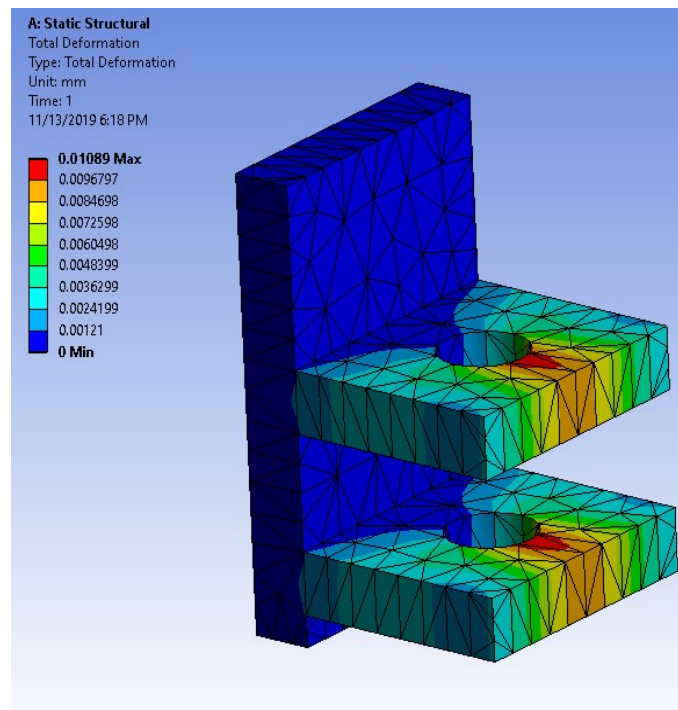


Figure 16: Clevis Deformation Under Load

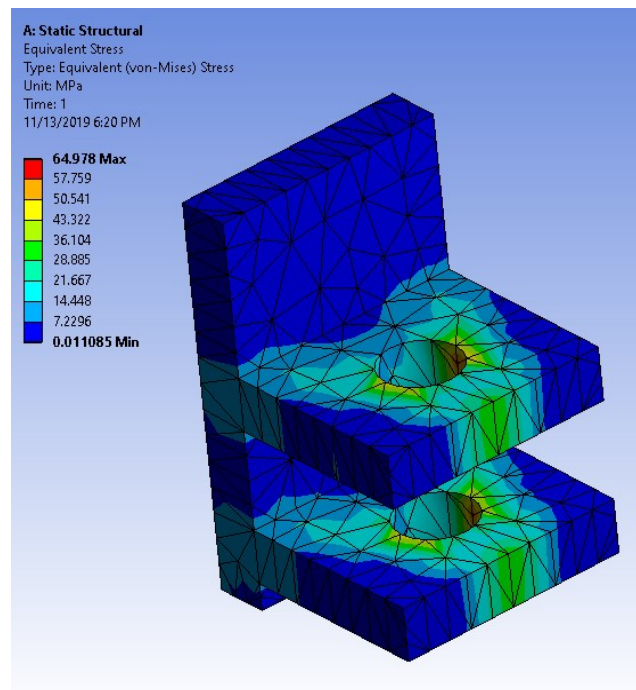


Figure 17: Von-Mises Stress in Clevis Under Load

This analysis was repeated using the same magnitude of the force; however, this analysis was performed with the clevis under compression. These analyses cover the range of loading possibilities expected by the clevis and are sufficient to ensure the integrity of the clevis.

5.1.3. Tuned Deformation of Upper Frame

A working load analysis was performed on a typical setup of a large cylindrical pill-shaped tank with an approximate diameter of one meter. The purpose of this analysis was to confirm the stiffness of each of the load cell supports is approximately equal under the given loading conditions. The tank in question consisted of two load-bearing rings placed at the extremity of the straight cylindrical section of the tank. These load-bearing rings were constructed out of aluminum 6061-T6 and coupled together by a set of 12-inch mild steel channel section to transfer the force generated to the load cells. The tank was assumed to exert a force due to gravity of 14 000N and was subject to several sets of loading parameters that mimicked the forces and torques experienced during a high acceleration test.

In the example shown below, an additional force of 12 500N was exerted in the positive X direction to replicate to force exerted by the acceleration of the stage. An additional torque of -1 500Nm about the Y-axis was introduced to simulate the scenario where the center of mass is not coincident with the plane of support. This torque may be generated in situations where the tank in question is not filled to the optimal level due to desired variations of the fill level in the tank during testing.

The forces and torques mentioned above were applied to the inside surface of the rings and dispersed evenly. The reaction force was provided by a fixed-support on the lower surface of the upper frame in place of the connection between the upper and lower frames. This setup can be seen below.

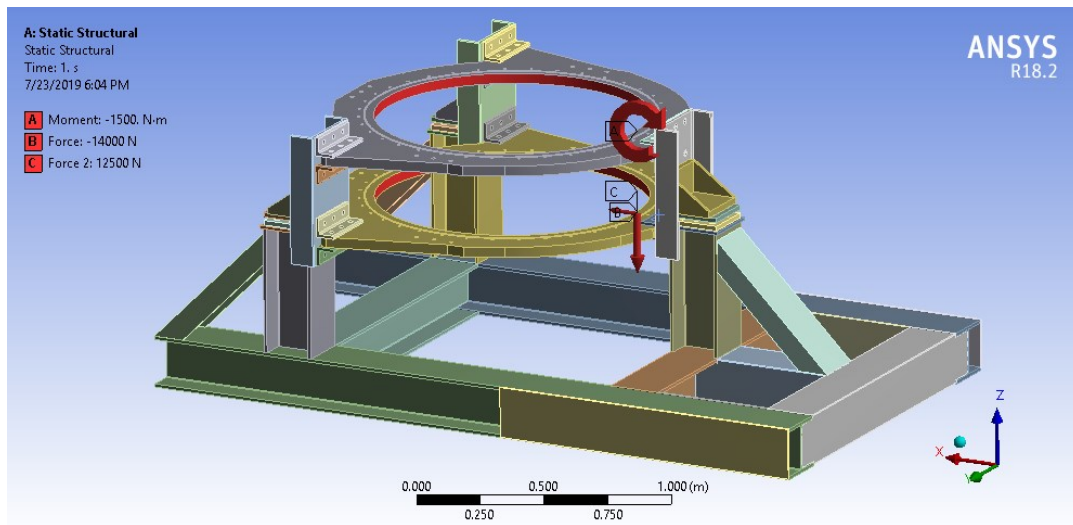


Figure 18: Upper Frame Load Analysis Configuration

This simulation produced the following results.

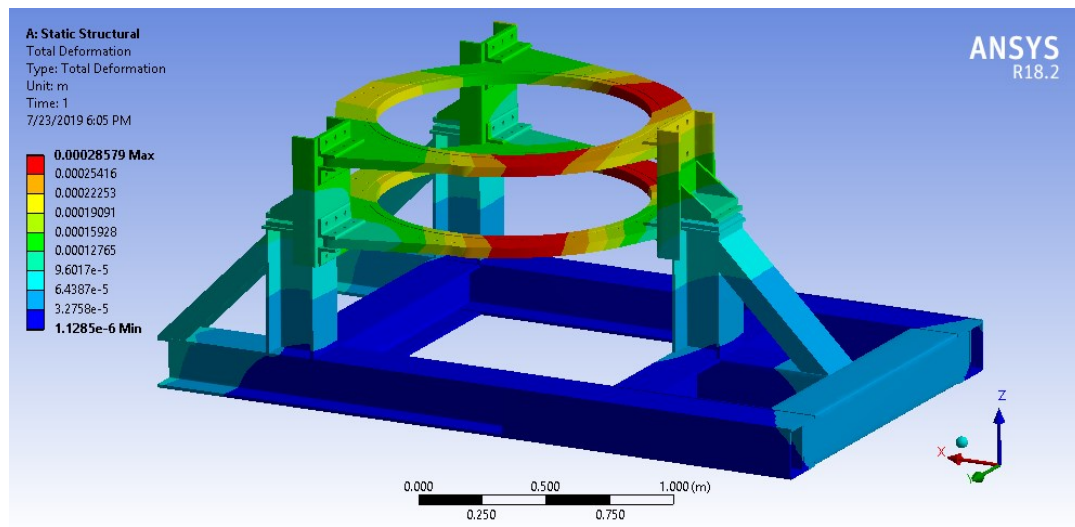


Figure 19: Upper Frame Deformation Under Load

The maximum deformation results in this case and all other cases tested were extremely small for a structure of this size showing a maximum deformation 0.286mm from rest. Despite the deformations in this model being extremely small, the very high stiffness of the ceramic load cell still allowed the possibility of uneven load distribution between the three load cells. In order to investigate this more thoroughly, a probe was inserted into the model at the upper surface of each load cell in the FEA model and the simulation re-analyzed. The results of these probes are shown in the table below.

Table 2: Upper Frame Load Cell Support Deflection under Load

	Displacement (mm)			Reaction Force (N)		
	X	Y	Z	X	Y	Z
Load Cell 1	0.099	0.000	-0.030	4235.2	-28.4	-5706.1
Load Cell 2	0.108	0.010	-0.011	4080.6	37.5	-4149.9
Load Cell 3	0.111	-0.002	-0.009	4164.3	-9.2	-4144.0

As seen in the table above, the reaction forces experienced by the load cells in the X-direction are very consistent between the load cells. This demonstrates the tuned nature of the support frame and the similar stiffness of each of the load cell supports. It must be noted that the reaction force in the Z direction is not similar across the three load cells. This is due to the torque applied to the system during the initial setup and is no cause for concern.

5.2. Emergency Containment Devices

The emergency containment devices are designed to prevent any part of the moving frame from exceeding its normal operating area in the event of a malfunction. These malfunctions include any loss of physical drive control resulting from broken or severed components as well as any software or firmware malfunction resulting in a case where the stage is being forced beyond the normal operating conditions of the system.

To meet these criteria, the containment devices will need to be capable of arresting the stage traveling at maximum actuator velocity with the stage carrying a maximum load. This case will result in the maximum kinetic energy of the stage calculated by:

$$KE_{max} = mv^2/2$$

$$KE_{max} = 4000kg * (2m/s)^2/2$$

$$KE_{max} = 8000J$$

The elastic modulus of the rubber pad can be calculated from the following formula:
(Larson n.d.)

$$E = \frac{0.0981(56 + 7.62336 * S)}{0.137505(254 - 2.54 * S)}$$

Where S is the ASTM D2240 Type A durometer rating of the rubber used, in this case, rubber with a durometer rating of 70 A was used.

$$E = \frac{0.0981(56 + 7.62336 * 70)}{0.137505(254 - 2.54 * 70)} = 5.5205MPa$$

The spring constant for a simple rectangular geometry of the south end pads can be estimated by:

$$k = \text{Elastic modulus} * \text{Area}/\text{length}$$

$$k_{south} = 5.5205 * 10^6 * \frac{2 * 0.203 * 0.228}{0.1143}$$

$$k_{south} = 4.47MN/m$$

Given the energy that is required to be absorbed, we can calculate the deformation of the rubber stop by:

$$PE = kx^2/2$$

From these, the deformation distance in the rubber pad can be calculated

$$x_{south} = \sqrt{2 * PE/k}$$

$$x_{south} = \sqrt{2 * 8000/4.47 * 10^6}$$

$$x_{south} = 0.0598m$$

Using a similar method for the north end pads

$$k_{north} = 8.49MN/m$$

$$x_{north} = 0.0434m$$

Assuming that the rubber pad will undergo pure elastic deformation before the stage comes to a complete standstill, the maximum force can be calculated at the maximum deflection of the rubber pad:

$$F_{max} = kx$$

$$\max(F_{south}) = 4.47 * 10^6 * 0.0598$$

$$\max(F_{south}) = 267.3kN$$

$$\max(F_{north}) = 8.49 * 10^6 * 0.0434$$

$$\max(F_{north}) = 368.5kN$$

Given these results, the endstops underwent finite element analysis using ANSYS to determine if failure would occur in the steel structure before the stage came to a standstill. The symmetry of the endstops allowed reduction of computation load by dividing the endstop over the plane of symmetry. Adding frictionless zero-displacement supports to the bisected surfaces mimics the reaction of the whole model. The endstops were set up as follows

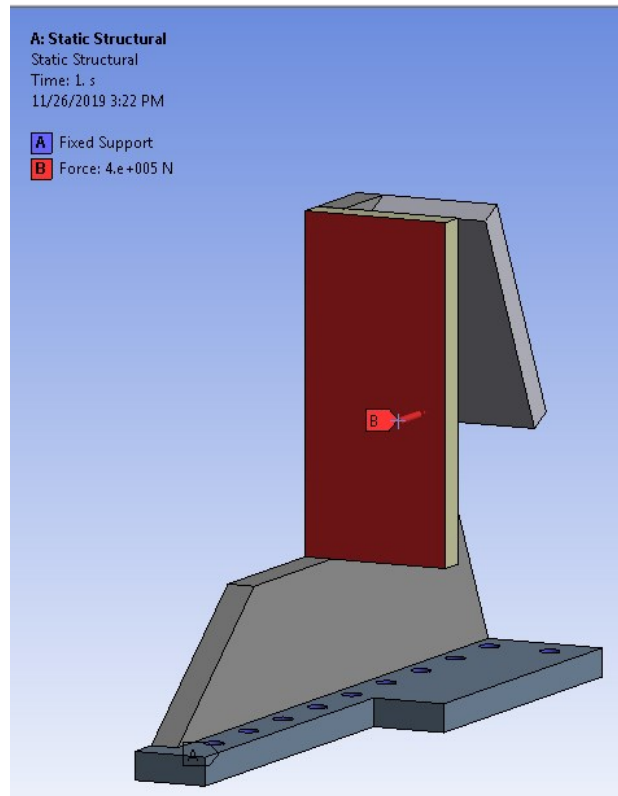


Figure 20: Emergency Containment Device Analysis Loading Configuration

The FEM model was solved and the results analyzed. This process was repeated making changes where the model was found to be lacking. After successive iteration, a design was chosen with the results shown below

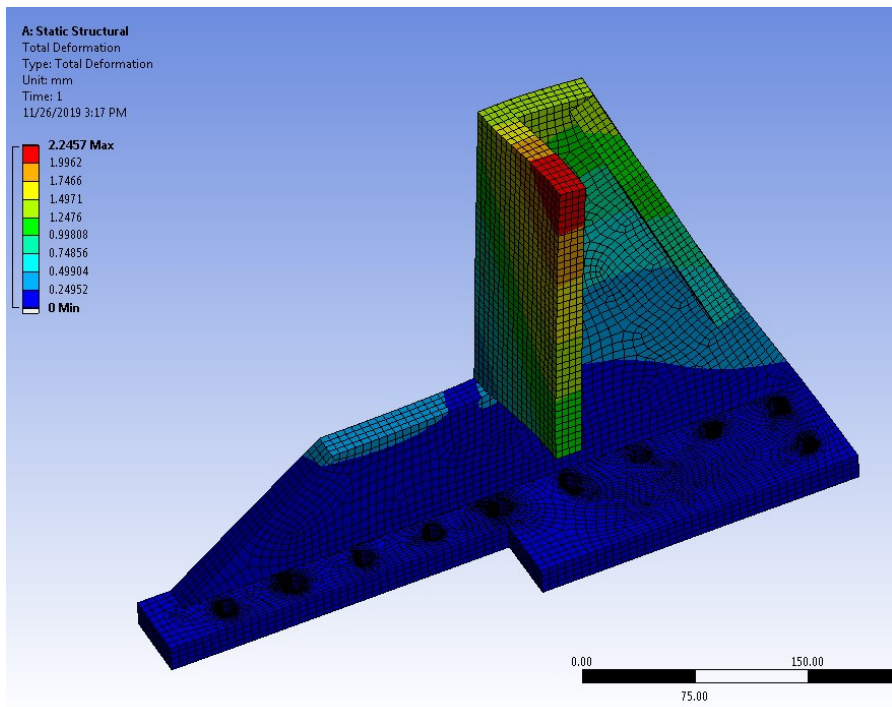


Figure 21: Emergency Containment Device Deformation Under Load

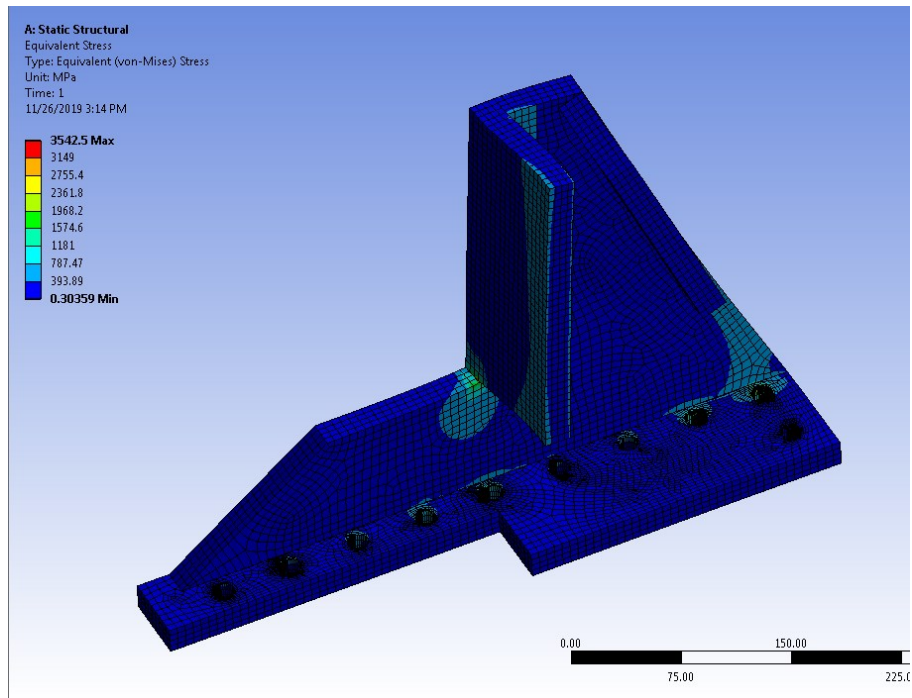


Figure 22: Von-Mises Stress in Emergency Containment Device Under Load

In the event that the stage does collide with the end stop, it is important to note that the center of mass of the moving component is significantly higher than the contact point between the frame and the endstop. This will cause a tendency of the stage to rotate over the end stop. As discussed in Chapter 4 – Motion interface, the linear rails, and bearings chosen for this application are not capable of restraining significant force in a direction upwards from the linear rail. The rotation generated by the hard stop will generate an upward force on the bearing opposite the collision. In this event, it is acceptable that the bearings fail and become dislodged from the rail; however, the frame must remain contained within the working area. To ensure this, we must determine whether that stage is capable of toppling over the endstop under any loading condition.

The increase of mass loading higher on the stage will increase the tendency of the stage to gain rotational momentum during the collision, thus, for the purpose of this analysis, we will examine the worst-case loading of the stage operating at full capacity loaded with the center of mass at the maximum height.

In a worst-case scenario, there will be a perfect momentum transfer from linear forward motion to rotational momentum around the fulcrum at the collision point. If this assumption is made, then we can calculate the upward velocity of the center of mass of the stage.

$$\Delta H = v^2/2g$$

This calculation needs to be performed for each test as it is not only dependant on the height of the load in question but also the X position of the center of gravity of the given setup.

Chapter 6 - Fabrication

6.1. Foundation

Before the foundation could be laid the main I-beams needed to be prepared. The I-beams were sent to a third party to have the upper surfaces skimmed to remove surface imperfections and distortions due to warping in the steel. During this process, the beams were first shimmed in the relaxed state before being clamped down on the opposing to avoid distortions due to spring back after machining. At the same time, mounting holes for the components were machined into the beams.

The main I-beams needed to be placed very precisely to prepare for the foundation to be poured. To do this, the hole was first prepared with a reinforcing bar and the beams were clamped to a pair of steel tubes and suspended over the hole where the foundation was to be laid. Using a set of jigs, laser levels and other instruments the beams were made to be parallel, straight and level to within 1mm. The image below shows the foundation during the process of leveling.



Figure 23: Preparation of Foundation for Concrete Slab

After the concrete had been fully cured, the hardened linear railers mounted on their supports were then positioned and partially bolted to the underlying beams. These bolts were intentionally left partially loose to allow for alignment later in the process.

6.2. Motor – Actuator Connection

The motor and actuator are connected via a steel box section with welded plates on each end and are responsible for holding the torque developed by the motor as well as partially holding the linear force developed by the linear actuator. This piece is of particular interest to us, as it needs to maintain a very tight tolerance during operation. The motor and actuator are connected via a bellows-type coupling. This coupling allows for a small amount of angular and radial misalignment; however, due to the highly cyclic nature of any deflection in the coupling, the deflection needs to be kept below 0.30mm according to the manufacturer (GAM 2015).

Due to the internal stress in the steel from the manufacturing process, as well as additional stresses caused during welding, we were not confident that during machining that some of these stresses would be released, thus causing the part to warp. To maintain the desired tolerances, the steel needed to be relaxed through the process of annealing. Annealing the crystalline structure to reform in an unstressed manner that would mitigate warping during the machining process. The steel was placed in an oven at 950°C for four hours to remove the crystalline structure. Afterward, the part was left to cool in the oven overnight to promote homogeneous cooling.

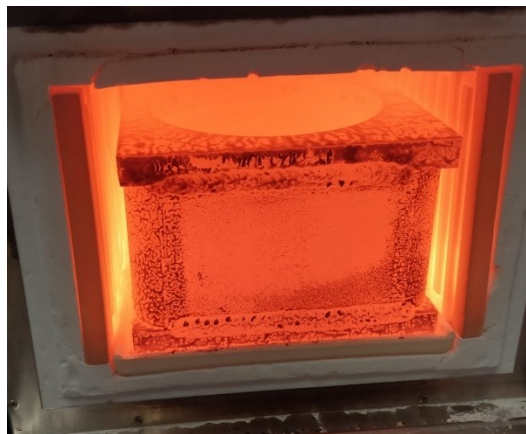


Figure 24: Motor-Actuator Connection Undergoing Annealing

Once the steel had cooled to room temperature the secondary machine processes took place. This brought the component into final dimensions without any risk of further distortions.

6.3. Lower Frame

The lower frame was manufactured in two parts. The main section of the frame was manufactured by welding the tube sections together on a flat surface to ensure a relatively flat finished product. The upper section was manufactured by welding a similar set of steel flat bar in the same manner. It is necessary the connection between the lower frame and the multipurpose frame relies on threaded insert nuts that are welded from the underside of the structure, an impossible feat in the tube sections. Once the insert nuts were welded in place the two segments of the frame were then welded together.

The steel blocks that are used to mount the linear bearing were then mounted to the frame. It is vital these blocks were placed straight and parallel, as the linear rails are very unforgiving to misalignment of the linear bearings. To achieve the concentricity required, the linear bearings were first mounted to the bearing support block and then the linear shafts were inserted into the bearings. The bearings and shaft were protected from splatter and the support blocks were welded into place ensuring that each set of bearings was colinear.

6.4. Linear Bearing and Rail Alignment

Alignment between the linear rails and bearings is vital to ensure the proper functioning of the linear stage. Misalignment could result in excessive loading of the linear components, which may result in a drastic reduction in the working life of these components. In a worst-case scenario, the bearings may bind resulting in instant catastrophic failure of the system.

To ensure proper alignment, the first step was to ensure the rails are both coplanar. This was established during the construction of the slab while the main beams were being placed. Fortunately, this is one of the less critical alignment parameters and does allow for very small deviations.

Secondly, a straight reference needed to be created. This reference was created by securing one of the linear rails. This would then become the reference and would not be moved or manipulated throughout the alignment process. Once the reference rail was secured, a tenths indicator was used to sweep the rails to check the perpendicular distance between the rails. The perpendicular distance between the rails is one of the more sensitive parameters and needed to be controlled tightly to ensure smooth operation.

The distance between the extremities of the rails was checked and adjusted. Once this dimension was within tolerance, the ends were then lightly bolted down and then rechecked and adjusted. This process was repeated until the ends of the rail was tightly secured. A measurement was made in the center of the rail to ensure the rails were parallel over their length. If any adjustment was necessary, then the rail was manipulated and tightened in place. The image below depicts the linear rails once they had been mounted, aligned and secure to the foundation.



Figure 25: Foundation with Linear Rails Mounted and Secured

Next, the linear bearings needed to be installed. The linear bearings are particularly sensitive to alignment during installation. Any misalignment would cause ball bearing to be ejected from their housing crippling the function of the bearing. As a result, each bearing was installed by hand and placed in its approximate location. The frame was then placed on top of the bearing and bolted into place.

The alignment of the bearing was then checked by feeling for resistance while manually moving the frame from one end to the other. Any resistance felt at this point would indicate excessive loading in the bearings caused by misalignment and the process would need to be repeated.

6.5. Emergency Containment Device

Components for the emergency containment devices arrived from suppliers which were water-jet cut to shape. They were then welded together, primed and painted. The rubber pads were formed by adhering layers of rubber sheet that was precut to shape. The ECDs were then firmly bolted into place on the main beams.

6.6. Upper Frame

The upper frame was fabricated from 12-inch steel I-beams that arrived from the supplier mostly precut to length except for the load cell support stiffeners that needed a 45° angle cut at each end. The two most critical aspects of the fabrication of the upper frame were ensuring the lower section remained flat and ensuring the location of the load cell mounts were located accurately.

The frame was kept flat during welding thanks to numerous precautions taken during the assembly process. First, the frame was laid flat on a surface that was known to be flat and tack welded together. The structural welding was then performed in a systematic manner that avoided excessive heating at any single location. As the welding progressed the continued and warping induced by the welding was corrected and then welding continued.

The location of the load cell mounts needed to be precise to within 3mm to allow for the slotted holes to align with the load cell mounting plates above. Fortunately, a large aluminum plate to be used in an upcoming test on the linear stage had a bolt pattern for the load cell mounts cut during the water jet cutting process. This plate was used as a jig and was bolted onto the load cell mounts to ensure the proper location of the load cell mounts.

Chapter 7 - Calibration

Calibration is an essential part of the testing process. It allows us to be confident in the measurements taken. To calibrate the system, measured loads will be applied to the system and the response of the system checked and corrected. Although each of the three sensors had been calibrated by Kistler, the system needs to be calibrated as a whole. This is because each time the load cells are placed on the stage, subtle differences in mounting and positioning will mean the force is transmitted slightly differently each time. Thus, confirming accurate results rely on accurate calibration.

The system incorporates three load cells that will each produce three sets of data, which are forces in the X, Y, and Z direction. The nine channels of data being output from the load cells need to be converted into the three primary forces and three primary torques. The six outputs will include three forces in the pure X, Y, and Z direction that are orthogonal, as well as three torques about these primary axes. To achieve this we need to produce a set of equations that are capable of converting a stream of nine channels of data into the six required channels. The set of equations below show how each force or torque applied to the system contributes to the output of each load cell. The following equations were derived from a report published describing the mathematics behind the Spinning Slosh Test Rig (Southwest Research Institute 2003).

$$\begin{aligned}
 V_{x1} &= K_{x1,Fx}F_x + K_{x1,Fy}F_y + K_{x1,Fz}F_z + K_{x1,Tx}T_x + K_{x1,Ty}T_y + K_{x1,Tz}T_z \\
 V_{x2} &= K_{x2,Fx}F_x + K_{x2,Fy}F_y + K_{x2,Fz}F_z + K_{x2,Tx}T_x + K_{x2,Ty}T_y + K_{x2,Tz}T_z \\
 V_{x3} &= K_{x3,Fx}F_x + K_{x3,Fy}F_y + K_{x3,Fz}F_z + K_{x3,Tx}T_x + K_{x3,Ty}T_y + K_{x3,Tz}T_z \\
 V_{y1} &= K_{y1,Fx}F_x + K_{y1,Fy}F_y + K_{y1,Fz}F_z + K_{y1,Tx}T_x + K_{y1,Ty}T_y + K_{y1,Tz}T_z \\
 V_{y2} &= K_{y2,Fx}F_x + K_{y2,Fy}F_y + K_{y2,Fz}F_z + K_{y2,Tx}T_x + K_{y2,Ty}T_y + K_{y2,Tz}T_z \\
 V_{y3} &= K_{y3,Fx}F_x + K_{y3,Fy}F_y + K_{y3,Fz}F_z + K_{y3,Tx}T_x + K_{y3,Ty}T_y + K_{y3,Tz}T_z \\
 V_{z1} &= K_{z1,Fx}F_x + K_{z1,Fy}F_y + K_{z1,Fz}F_z + K_{z1,Tx}T_x + K_{z1,Ty}T_y + K_{z1,Tz}T_z \\
 V_{z2} &= K_{z2,Fx}F_x + K_{z2,Fy}F_y + K_{z2,Fz}F_z + K_{z2,Tx}T_x + K_{z2,Ty}T_y + K_{z2,Tz}T_z \\
 V_{z3} &= K_{z3,Fx}F_x + K_{z3,Fy}F_y + K_{z3,Fz}F_z + K_{z3,Tx}T_x + K_{z3,Ty}T_y + K_{z3,Tz}T_z
 \end{aligned}$$

Where V_{x1} represents the X-component of the force output by the load cell in position one, the F_y denotes the Y-component of force on the system and the $K_{z3,Ty}$ denotes the constant that relates the Z-component of the third load cell to the torque about the Z-axis.

Given that the layout of the system is consists of the three sensors mounted in a single plane and the load cell in position one is coincident with the X-axis of the system, then the following six equations can be derived through careful consideration.

$$V_{Fx} = V_{x1} + V_{x2} + V_{x3}$$

$$V_{Fy} = V_{y1} + V_{y2} + V_{y3}$$

$$V_{Fz} = V_{z1} + V_{z2} + V_{z3}$$

$$V_T = V_{z2} - V_{z3}$$

$$V_{Ty} = V_{z1} - (V_{z2} + V_{z3}) \frac{\Delta x_3}{\Delta x_1}$$

$$V_{Tz} = (V_{x2} + V_{x3}) \frac{\Delta y_3}{\Delta x_1} - V_{y1} + (V_{y2} + V_{y3}) \frac{\Delta x_3}{\Delta x_1}$$

These equations can be substituted into the set of equations above and then condensed into matrix form as follows.

$$\begin{bmatrix} V_{Fx} \\ V_{Fy} \\ V_{Fz} \\ V_{Tx} \\ V_{Ty} \\ V_{Tz} \end{bmatrix} = K \begin{bmatrix} F_x \\ F_y \\ F_z \\ T_x \\ T_y \\ T_z \end{bmatrix}$$

Given the above matrix form of the equation, we are conveniently able to invert the K matrix which allows us to calculate to forces and torques on the given system from the output force of the load cells using the following equation.

$$\begin{bmatrix} F_x \\ F_y \\ F_z \\ T_x \\ T_y \\ T_z \end{bmatrix} = K^{-1} \begin{bmatrix} V_{Fx} \\ V_{Fy} \\ V_{Fz} \\ V_{Tx} \\ V_{Ty} \\ V_{Tz} \end{bmatrix}$$

To use this equation above, one must be able to calculate the values in the K matrix. These values are most easily calculated by the isolation of forces and torques on the system. By doing this the terms not associated with the isolated value can be set to zero and thus removed from the system. This approach allows the calculation of each of the K values in the system by systematically applied a load that produced an isolated response from the system for each of the six fundamental loads.

To produce the pure loads needed to calculate the K-matrix, a series of configurations have been devised that will load the apparatus with a single primary load while keeping the rest as near zero as possible.

It is important to note during the creation of these forces that the load cells being used generate a charge as the applied load changes. This charge that is generated leaks over time therefor measurements need to be taken soon after the change in load. This presents a challenge because the setups required to produce pure torques involve the balancing of two forces applied at a distance from the center. The balancing of these torques takes time to set up and balance during which time the charge in the load cells will decay. To solve this problem, a unique solution was used whereby the measurement was not taken during the loading phase, but rather the load was applied and then the measurement was taken shortly after the reduction of the load. This solution allows the operator time to carefully assure the loading of the apparatus is done precisely without fear of loss of accuracy due to charge decay.

To produce accurate repeatable force, the force will be produced by hanging weight. This force, however, needs to be redirected. This will be done through a set of pullies to direct and align the forces in the required direction. The use of a pulley has some disadvantages. Mainly, the introduction of friction reduces the effective force produced by the hanging weights. To combat this, a set of calibrated independent load cells will be used to measure the force applied by the hanging weights. It is important to note that these load cells must be placed between the apparatus and the first pulley such that the correct force is measured.

In some cases, a force needs to be equally split into two separate locations. To do this a section of T-slot aluminum framing is used as a yoke to equally divide the forces. The

T-slots in the frame proved to be particularly useful as small adjustments could be made by sliding the connection points.

7.1.1. X-Force Calibration

The X-Force calibration was conducted by hanging a set of weights off a pulley. The force was redirected over a pulley and then distributed through a yoke. The setup seen below was then repeated by moving the pulley support frame to the opposite end of the stage.

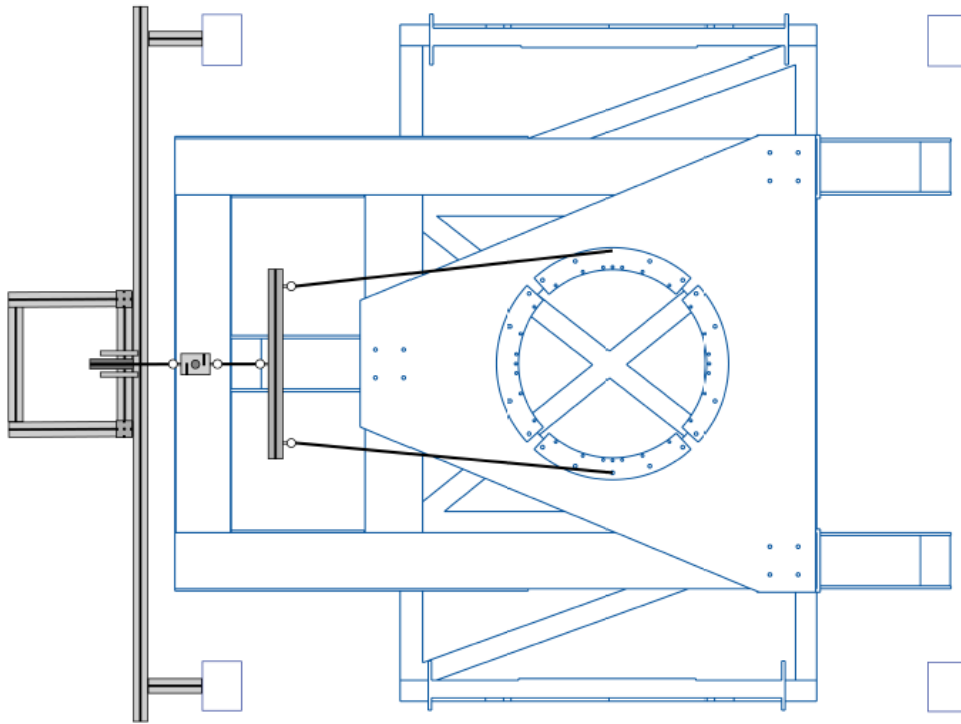


Figure 26: X-Force Calibration Setup

7.1.2. Y-Force Calibration

The Y-force calibration was achieved using a similar setup as the X-force calibration setup. However, this time the force needed to be redirected through two pulleys to ensure a pure Y-force. Similarly to the X-force calibration, this calibration procedure was repeated in the opposite direction.

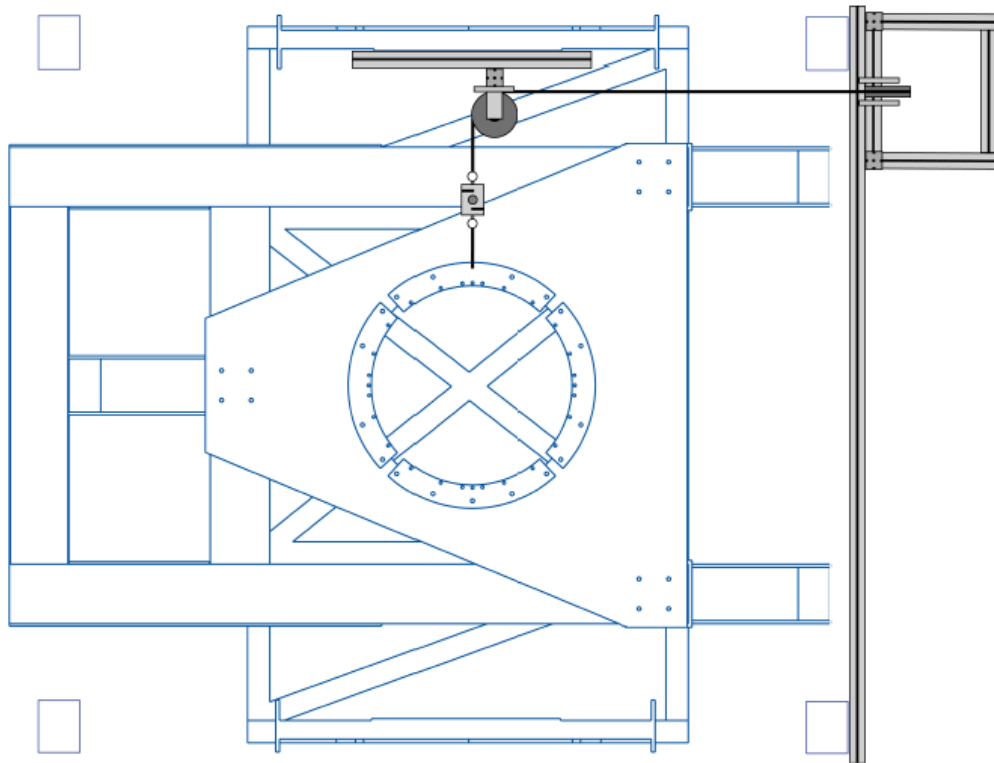


Figure 27: Y-Force Calibration Setup

7.1.3. Z-Force Calibration

The Z-Force calibration uses two pulleys to redirect the force from the hanging weight to the center location of the supposed tank to be tested.

The opposing Z-force calibration was performed differently. Fortunately, the two-ton overhead crane that was used to place the heavy components in place was able to be used not only as an anchor point but also was used to apply the force required for calibration. This avoided the need to hang weights. The crane was used to apply an approximate load to the system, while a turnbuckle in line with the system was used to fine-tune the load to the required loading.

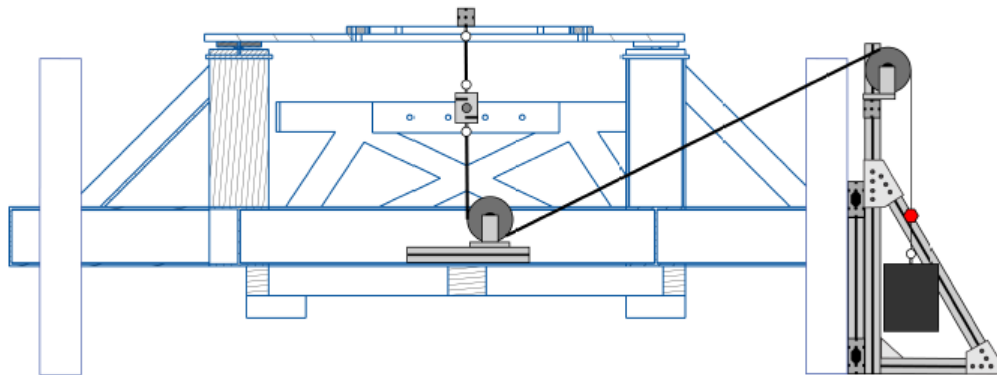


Figure 28: Z-Force Calibration Setup

7.1.4. X & Y-Torque Calibration

Torque calibration differed significantly from the direct force calibration setups. During torque calibration setups, there need to be two forces applied to the apparatus, which need to be of equal magnitude acting in opposite directions equally separated from the axis which they torque about.

These calibrations were more tedious than force calibrations as not only did the load need to be set precisely, but the load also had to be distributed evenly between the two

contact points. This process was made more difficult due to the dissymmetry caused by the friction in the pulley used to redirect the force.

To ensure the forces were distributed across the yoke evenly, taking account for the friction introduced by the pulley, two calibrated load cells were used to ensure the loads applied were exactly equal.

Additionally, complications arose when the yoke used to distribute the load tended to fall to one side or the other as a result of tension release from the overhead crane. This results in a small residual force being applied to a single loading point. This was dealt with by ensuring that, prior to loading, the yoke was perfectly balanced and thus resulting in no residual loads.

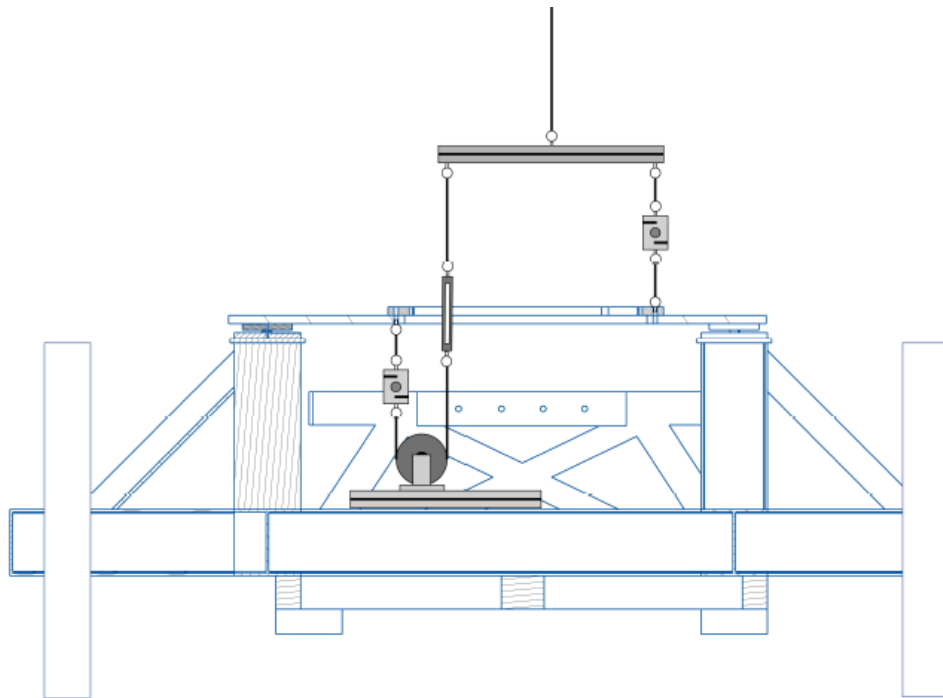


Figure 29: X and Y Torque Calibration Setup

7.1.5. Z-Torque Calibration

The Z-axis calibration returns to the use of the hanging weights. In this configuration, the tension in the cables is divided by a yoke to ensure equal splitting of the tensions. Each cable is then routed around a pulley to a contact point located equidistant from the center of the tank, but with the force vector in opposing directions.

The weight of the yoke again posed an added complication. When the tension has been released the weight of the yoke hanging provided a residual force. To combat this issue, a table was placed below the yoke such that the yoke rested on the table when the tension was released from the cable.

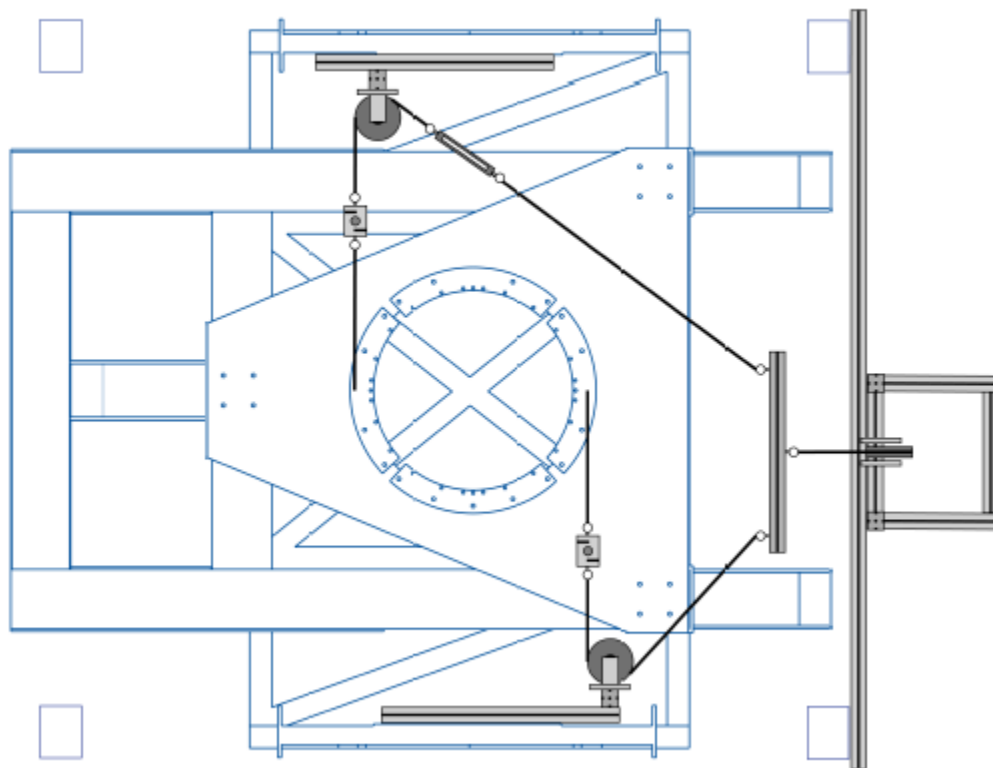


Figure 30: Z-Torque Calibration Setup

Chapter 8 - Demonstration

Testbed sprung to life on April 11, 2020, to perform its first sinusoidal test. The initial tests were conducted at low frequencies and small amplitudes to assess the stages was working as expected before progressing to more demanding tests.

8.1. Complete System Overview

The system came to be completed with no major deviations from the final design. The assembly process was relatively smooth with no major alterations needing to be made.



Figure 31: Complete Linear Stage Overview



Figure 32: Completed Linear Stage Front View

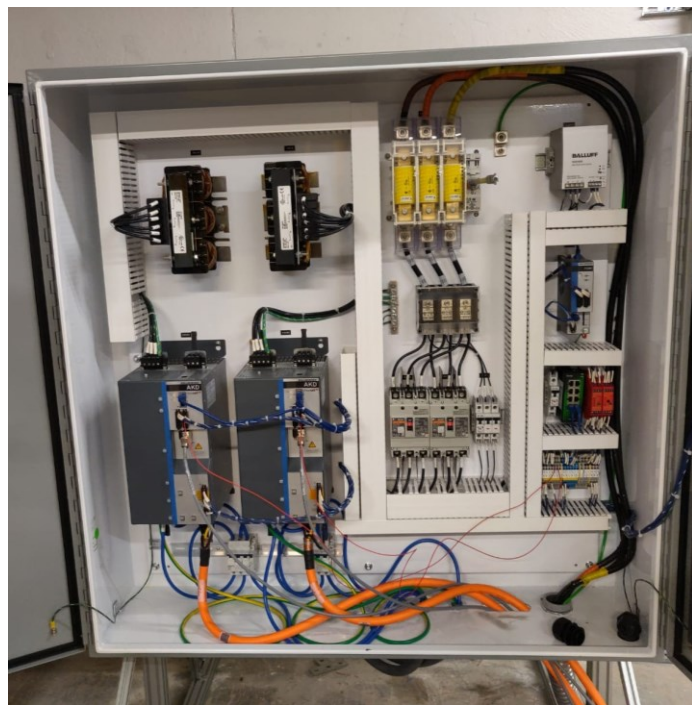


Figure 33: Completed Control and Instrumentation Panel

8.2. Human-Machine Interface

The human-machine interface allows the user to operate the machine via an ergonomic touch screen display. The screen capture below shows the main navigation screen. From this screen, the user is able to access all the features of the system including homing, manual jogging, coordinated manual jogging, and automated stage controls.

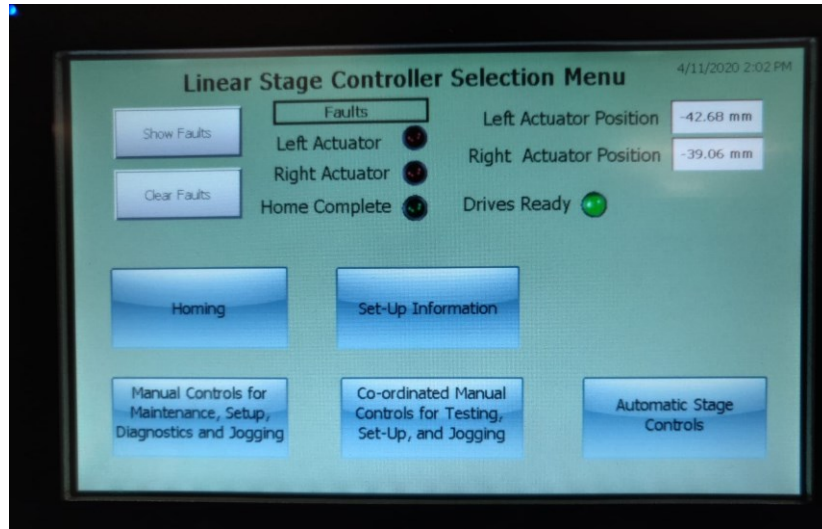


Figure 34: HMI Main Navigation Screen

The screen below shows the interfaced used to program the automated stage controls. From this screen, the user can select the parameters of the waveform to be performed.

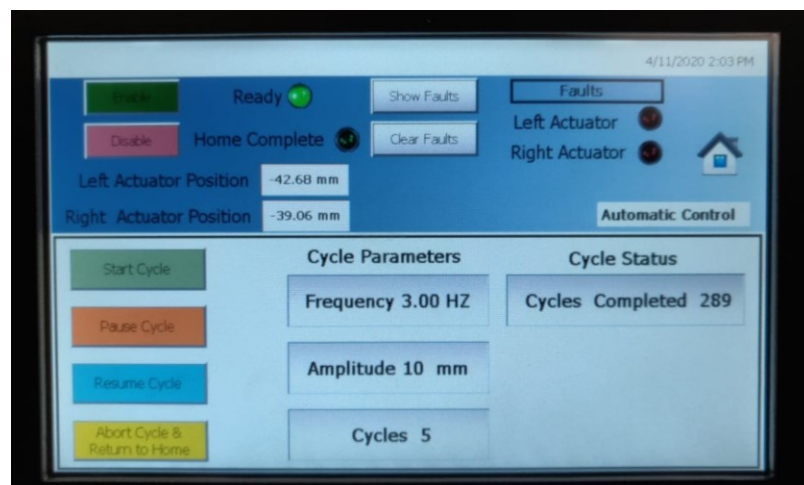


Figure 35: HMI Automated Stage Controls

Chapter 9 - Conclusion and Future Work

In conclusion, the development of high-performance linear stages is crucial to the increased understanding and verification of multiphase fluid slosh. The high capabilities of the linear stage presented in this thesis will become a great asset to the Florida Tech Center for Advanced Manufacturing and Innovative Design (CAMID) and the research being performed there. The versatility of this linear stage will be advantageous to reduce the time and costs of development associated with slosh testing of tanks by taking advantage of the modular design to reuse components as the stage is prepared between tests.

The linear stage has now been completed and is currently undergoing trials to verify its performance capabilities and will soon be fully operational.

This stage looks forward to both a bright and busy future as the first of many analyses and tests are being prepared for testing upon it. This linear stage will be used in the near future to test the high-frequency response of a diaphragm being used on NASA's Plankton, Aerosol, Cloud, ocean Ecosystem mission (PACE) (NASA n.d.). It will be launched in 2020 and will survey the earth to help monitor and address new and emerging science questions.

References

- Abramson, H. N. 1966. *The Dynamic Behavior of Liquids in Moving Containers, with Applications to Space Vehicle Technology*. Technical Report, NASA.
- Bruno, Tory, interview by Destin Wilson Sandlin. 2020. *How Rockets are Made* (February).
- Dodge, Franklin T. 2000. *The New "Dynamic Behavior of Liquids in Moving Containers"*. Technical Document, Southwest Research Institute.
- G. Lapilli, J. Sargent, M. Rhoney, H. Gutierrez, D. Kirk, B. Wise, W. Tam. 2016. *DESIGN AND DEVELOPMENT OF 2,000 KG LINEAR SHAKER PLATFORM FOR SPACECRAFT PROPELLANT TANK SLOSH BEHAVIOR VALIDATION AND RESEARCH*. Melbourne: Florida Institute of Technology.
- GAM. 2015. "KM Series Bellows Coupling." *GAM*.
<https://dpk3n3gg92jwt.cloudfront.net/domains/gam/pdf/KM.pdf>.
- Kollmorgen. n.d. "<https://www.kollmorgen.com/>." *Kollmorgen*. Accessed 4 2020.
<https://www.kollmorgen.com/en-us/service-and-support/knowledge-center/literature-overview/>.
- Larson, Kent. n.d. *The Dow Chemical Company*.
<https://www.dow.com/content/dam/dcc/documents/en-us/tech-art/11/11-37/11-3716-01-durometer-hardness-for-silicones.pdf?iframe=true>.
- NASA. n.d. *Plankton, Aerosol, Cloud, ocean Ecosystem* . Accessed 04 09, 2020.
<https://pace.oceansciences.org/about.htm>.
- Ran Zhou, Michael Vergalla, Sunil Chintalapati, Daniel Kirk and Hector Gutierrez. 2012. *Experimental and Numerical Investigation of Liquid Slosh Behavior Using Ground Based Platforms*. AIAA Journal of Spacecraft and Rockets.
- SKF. 2014. "Linear Bearings and Units." *www.SKF.com*.
<https://www.skf.com/group/support/splash>.

Southwest Research Institute. 2003. "NUTATION TIME CONSTANT MODEL PARAMETERS FOR THE STEREO SPACECRAFT." Final Report.

Thomson Linear. n.d. "Precision linear Actuators." *Thomson Linear*.

https://www.thomsonlinear.com/downloads/actuators/Precision_Linear_Actuators_CTEN.pdf.

Vaishnav, D., Dong, M., Shah, M., Gomez, F. et al. 2014. "Investigation and Development of Fuel Slosh CAE Methodologies." *SAE International* 278-288.

Appendix - Actuator Alignment

As previously noted the alignment between the linear actuator and the linear rails that the stage rides on is critically important. This appendix will examine the procedures used to align the actuators with the linear rails.

To check the alignment, a tenths indicator is used to measure very small changes in distance between the stage and the linear actuator.

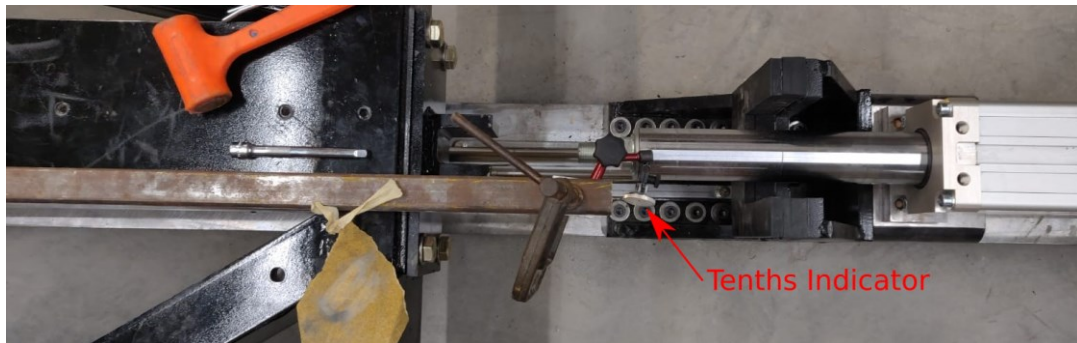


Figure 36: Overhead View of Indicator

The picture above shows a birds-eye view of the setup used to support the indicator during alignment. The procedure is conducted as follows:

1. Both actuators are disconnected from the stage by removing the pin from the clevis.
2. The actuator not being examined is fully retracted.
3. The actuator being examined is extended such that there are roughly 6 inches of the polished shaft exposed beyond the emergency containment device.
4. A tenths indicator is then placed in a position such that the needle is running along either the left or the right-hand side of the shaft. This may require the use of an object to extend the reach of the indicator, in the example above a section of steel was clamped to the stage.
5. The indicator is adjusted such that it is in firm contact with the shaft.
6. The stage is then pushed by hand back and forth allowing the indicator to sweep over a 6-inch range.
7. Measurements are taken at each end of the stroke to assess the parallelity of the actuator.

8. If the actuator is found to be out of alignment the bolts on the actuator mount must be loosened and the actuator is realigned. These can found located beneath the actuator as indicated in the image below.

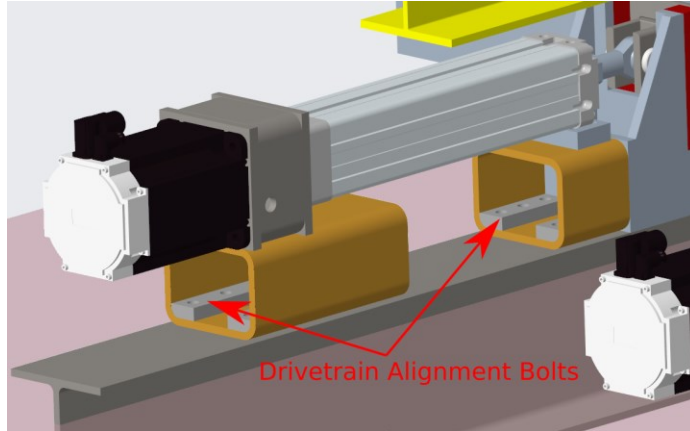


Figure 37: Drivetrain Alignment Bolts

9. These steps are repeated until the actuator is within tolerance.
10. This procedure must be repeated on both actuators to ensure alignment.

After the stage was assembled this alignment procedure was performed and the initial alignment figures are shown below.

Table 3: Initial Alignment Figures

<u>Actuators</u>	<u>North (in)</u>	<u>South (in)</u>	<u>Deviation (in)</u>	<u>Angular misalignment (°)</u>
East	0.0100	0.0090	0.0010	0.0002
West	0.0090	0.0070	0.0020	0.0003